Università degli Studi di Ferrara

DOTTORATO DI RICERCA IN
"Farmacologia ed Oncologia Molecolare"

CICLO XXIV

COORDINATORE Prof. Antonio Cuneo

Anti-miR-135b in colon cancer treatment

Settore Scientifico Disciplinare BIO/11

Dottorando
Dott. Valeri Nicola

Tutore
Prof. Volinia Stefano

Anni 2009/2011

Index

Abstract (English)

Background: MicroRNAs (miRs) are small non coding RNAs involved in cell homeostasis. miRs are deregulated in colorectal cancer (CRC). Our study aimed at identifying miRs with a driver role in carcinogenesis altered by similar mechanisms in both human and mouse CRC. Goal of the study was to use CRC mouse models for the pre-clinical development of anti-miRs as therapeutic drugs. **Methods:** Azoximetane (AOM)/Dextran-Sulfate (DSS) treated mice or CDX2Cre-APC f/wt mice were used to study inflammation-associated and sporadic APC-related CRC. Human Inflammatory Bowel Disease associated (n=15), and sporadic (n=62) CRC with their matched normal tissues were collected according to Good Clinical Practice recommendation and subjected to RNA extraction using Trizol. miR and gene expression profiling was assessed by nCounter technology (Nanostring Seattle). Anti-miR-135b and scrambled probes for in vivo studies were synthesized by Girindus. **Results:** miRs profiling from AOM/DSS and CDX2Cre-APC f/wt CRC revealed that miR-135b is one of the most up-regulated miRs in both models. In humans miR-135b over-expression was found in both IBD and sporadic CRC and was associated with reduced Progression Free Survival and Overall Survival in CRC patients. Molecular studies in Mouse Embryo Fibroblast and human CRC cell lines highlighted the role of two major pathways in the upstream activation of miR-135b: APC-β-Catenin and SRC-PI3K. MiR-135b up-regulation resulted in reduced apoptosis and increased cell growth due to the down-regulation of TGFRB2, DAPK1, APC and FIH. Silencing of miR-135b in vivo reduced tumor multiplicity and tumor load in the AOM/DSS CRC model. Mice treated with anti-miR-135b showed well differentiated tumors and acinar pattern while tumors in the control groups showed low differentiation and adenomatous pattern. **Conclusions:** Our data suggest that miR-135b is a key molecule whose activation is downstream of oncogenes and oncosuppressor genes frequently altered in CRC. Our study defines specific pathways that converge on the

activation of the same microRNA. The “in vivo” silencing of miR-135 shows preclinical efficacy with low toxicity and represents the first in vivo study for the use of anti-miRs in CRC treatment

Abstract (Italiano)

Introduzione: I MicroRNAs (miRs) sono dei piccoli RNA non codificanti coinvolti nell'omeostasi cellulare. L'espressione dei miR e' deregolata nel tessuto tumorale dei pazienti affetti da cancro del colon retto. Il nostro studio e' volto ad identificare microRNA implicati nella cancerogenesi del colon la cui espressione sia influenzata da meccanismi genetici simili nel topo e nell'uomo. Obiettivo dello studio e' quello di usare modelli murini di cancro del colon per lo sviluppo pre-clinico di terapie basate sull'impiego di anti-miR. **Materiali e Metodi:** Modelli murini di cancro del colon associati alla somministrazione di Azoximetane (AOM)/Dextran-Sulfate (DSS) o alla presenza di mutazioni di APC nel colon sono stati usati come modelli per il cancro del colon associato ad infiammazione o sporadico. Tessuti tumorali di cancro del colon associati a malattie ulcerose croniche o di tumori sporadici e i rispettvi tessuti normali adiacenti sono stati collezionati secondo le norme di Good Clinical Practice e sono stati sottoposti ad estrazione di RNA. Il profilo di espressione dei microRNA e' stato valutato mediante nCounter technology (Nanostring Seattle). Oligonucleotidi Anti-miR-135b o controllo per gli studi in vivo sono stati sintetizzati da Girindus Inc. **Risultati:** Il profilo di espressione dei microRNA nei due modelli murini sopraindicati ha identificato il miR-135b come uno dei microRNA maggiormente espressi in entrambi i modelli. In campioni di cancro umano il miR-135b e' risultato iper-espresso sia nel cancro sporadico sia in quello associato a malattie infiammatorie croniche intestinali ed e' risultato associato a ridotta sopravvivenza. Studi in vitro in fibroblasti embrionali di topo e linee cellulari umane di cancro del colon hanno dimostrato che il miR-135b e' attivato da due sistemi di trasduzione del segnale frequentemente affetti da mutazioni nel tumore del colon: APC-β-Catenina e SRC-PI3K. L'iper-espressione del miR-135b in linee cellulari umane era associata a ridotta apoptosi e aumento della crescita cellulare a causa dell'inibizione di numerosi geni onco-soppressori: TGFRB2, DAPK1, APC ed FIH.

L’inibizione del miR-135b in vivo e’ risultata in una riduzione del numero e del volume tumorale. I tumori dei topi trattati con anti-miR-135b risultavano ben differenziati e con pattern acinare mentre quelli dei topi del gruppo di controllo apparivano scarsamente differenziati e con pattern adenomatoso. **Conclusioni:** I nostri dati mostrano che il miR-135b e’ un importante onco-miR la cui attivazione e’ legata alla presenza di mutazioni frequentemente osservate nel cancro del colon. Il nostro studio identifica quali vie di trasduzione del segnale convergono nell’attivazione dello stesso microRNA. L’impiego di anti-miR-135b mostra buona efficacia e scarsa tossicità e rappresenta il primo studio in vivo per l’impiego di anti-miR come strategia terapeutica in un modello murino di cancro del colon.

Introduction

ColoRectal Cancer (CRC) arises trough the progressive accumulation of mutations in oncogenes and onco-suppressor genes[1]. Targeting driver oncogenes or using mutations as biomarkers for response to treatment represent the best option to tailor cancer treatment[2]. Inhibitors of mutated oncogenes such as protein kinases have been developed and are currently used in clinical practice or under investigation in clinical trials[3]. Targeting driver oncogenes in CRC is associated to increased Time To Progression and Overall Survival (OS) in metastatic CRC patients[3]. Even though promising this approach has two main pitfalls: 1) response to target therapies is limited in time because drug resistance arises as a result of the activation of collateral pathways[4]. 2) while specific inhibitors of driver onco-genes can be developed and exploited into drug development, targeting lost onco-supressor genes such as the Adenomatous Polyposis Coli (APC) remains challenging to translate into therapeutic weapons.

microRNAs (miRs) are a class of small non-coding RNAs (19-25nt in length) involved in cell homeostasis and carcinogenesis[5]. Several miRs are aberrantly expressed in colorectal cancer and their deregulation has been linked to CRC progression and clinical outcome[6]. Different oncogenic pathways can merge on the same miR, as well as a single miR can control a general transcriptional program affecting dozens of target genes [5]. Since miRs often act as downstream effectors of protein kinases or driver genes mutated in cancer[7], targeting miR might represent a strategy to increase targeting specificity and overcome drug resistance. Furthermore the relative ease by which deregulated miRs can be detected in biological specimens from CRC patients increases the feasibility of this approach and its potential to be translated into a clinical setting[8]. Data on the efficacy of miR inhibition are available to date and prompt the use of anti-miR technology in CRC treatment in vivo [9].

Results

Target selection

In order to test which miRs are regulated in vivo by activating or inactivating mutations frequently occurring in CRC we ran a microRNA profiling on tumor and normal matched tissues from two different mice models of CRC. The CDX2P-NLS Cre;$Apc^{+/loxP}$ (CPC;Apc) model is characterized by the presence of a truncating mutation affecting one APC allele[10]. The APC inactivation promotes the formation of an average of 5 to 8 tumors in the colon and rectum, 1 tumor in the cecum and 2-3 tumors in the distal small intestine in six months old mice[10]. The Azoximehtane (AOM)/Dextran Sulphate Sodium (DSS) model is due to the synergic effect of the pro-carcinogen AOM associated to the intermittent administration of the inflammatory stimuli exerted by the pro-inflammatory drug DSS[11]. This model is frequently associated to mutations in the PI3KCA, KRAS and SRC pathways. AOM/DSS mice develop an average of twenty polyps mainly in the distal colon after 11 weeks of treatment[11,12]. β-catenin mutations in exon 3 have been described after AOM/DSS administration and depends often on the mouse strain used[13]. We sequenced exon 3 in the polyps of our AOM/DSS treated mice and no mutations were found. We used nCounter technology to run a genome-wide miR expression profiling in tumors and matched normal tissues from six mice for each model, CPC;APC and AOM/DSS. Both models have been developed using the C57BL6 strain allowing direct comparison between the two and avoiding biases due to different strains. Seventy-six miRs were aberrantly expressed in polyps from the CPC;APC model with $P < 0.01$, with 16 miRs increased and 17 decreased by greater than two fold. In the AOM/DSS model 94 miRs were aberrantly expressed in polyps compared to normal tissues with $P < 0.01$; among these, 15 miRs were increased and 9 decreased by greater than two fold (Figure 1). We focused on over-expressed miRs because we believe they have a stronger driver role in carcinogesis, and because silencing technologies

proved to be more effective than re-expression approaches mediated by lentiviral delivery[9]. miR-135b was found as one of the most over-expressed miR in both models (Figure 1). Real Time-PCR validation confirmed the over-expression of miR-135b in both the CPC;APC(fold change cancer/normal: 8.6; p: 0.0061) and the AOM/DSS model (fold change cancer/normal: 7.5; p value 0.031). In order to test whether inflammation itself was able to induce the over-expression of miR-135b we included in the validation analysis colon mucosa from mice treated with short (7 days) or long (78 days) DSS alone. DSS alone did not affect miR-135b expression leading to speculate that the AOM pro-carcinogenetic stimulus is fundamental for miR-135b up-regulation. Further confirming this hypothesis, normal tissues from AOM/DSS mice showed increased miR-135b expression compared to normal tissues from untreated or CPC;APC mice ($p < 0.0001$ for both comparisons) (Figure 2A).

In situ hybridization (ISH) analysis revealed that miR-135b is strongly expressed in cytoplasm from dysplastic cells in both mouse models. Faint signal was also detected in inflammatory cells and normal epithelial cells from the intestinal cryptae (Figure 2B).

MiR-135b is over-expressed in Human CRC

MiR-135b has been consistently reported as up-regulated in cancer compared to normal tissue [14-18]. We validated these observations by testing miR-135b expression in both sporadic and inflammatory bowel disease (IBD)-associated CRCs. Sixty-two sporadic CRCs were analyzed for miR-135b expression by RT-PCR. In line with data observed in mice[19] and previous reports in humans[14-18], miR-135b was up-regulated by an average 4 fold change in cancer compared to paired tissue ($p<0.0001$) (Figure 3A). When miR-135b was plotted against the tumor stage, miR expression correlated with tumor progression as it was increased in the sequence from Stage I to Metastatic Stage IV CRC (Figure 3B). The second analysis was performed in two independent sets of IBD-associated CRCs. In the first set of patients a paired analysis showed miR-135b up-regulation

in cancer compared to normal tissues (fold change 5.6; p: 0.0003) (Figure 3C). These findings were confirmed in the second set where miR-135b was also over-expressed in dysplasia compared to normal tissues suggesting that miR-135b deregulation might be an early event in colon carcinogenesis (mean fold change 7.15; p:0.0057) (Figure 3D). ISH showed that miR-135b is expressed in cytoplasm of epithelial cells, while stromal cells show very weak signal. Normal colic epithelia do express miR-135b mainly in the cryptae suggesting a role for miR-135b in cell proliferation. Dysplasia and invasive CRCs show a very strong miR-135b signal compared to normal adjacent tissues confirming our previous RT-PCR data (Figure 3E).

MiR-135b is associated with poor prognosis in sporadic CRC

In order to test if miR-135b can be associated to clinical outcome in CRC patients we plotted Kaplan–Meier survival curves for survival distributions and we compared them with the use of the Mantel–Cox log-rank test and the Wilcoxon test. Tumor stage, nodal status and miR-135b expression were identified as prognostic markers (Figure 4&5). The logarithmic ratio between miR-135b expression in cancer and normal tissue for each patient was used for the analysis. Patients were stratified in two groups according to miR-135b expression: *high* if miR-135b expression >2, and *low* if miR-135b expression $\leq$ 2. High miR-135b expression was associated to poor OS in the entire cohort of patients (p: 0.0044) and to poor Progression Free Survival (PFS) (Figure 5). A subgroup analysis in patients with stage II CRC identified a trend toward a worse prognosis for patients with high miR-135b. However, the difference was not statistically significant (p: 0.055) likely due to the small sample size (Figure 5D). A multivariate analysis confirmed miR-135b as an independent prognostic factor associated to OS.

MiR-135b over-expression is associated to mutations in specific CRC pathways

Data generated in mice suggested that miR-135b over-expression might be due to the involvement of several pathways. APC is the major player in the CPC;APC model[10] while different pathways might be involved in the AOM/DSS model[12]. In order to confirm that miR-135b over-expression is due to APC loss we re-induced APC by transfecting a plasmid encoding the APC full coding sequence (CDS) in the SW480 human CRC cell line, which harbors a mutated APC isoform[20]. Re-expression of Wild-Type (WT) APC caused a 6.8 fold change in APC expression (p:0.0338) and was able to cause a 48% reduction in miR-135b expression (p: 0.0063) after 12h. On the contrary inhibition of APC by siRNA in two different normal colon epithelial cell lines, NCM4060 and NCM 356,[21] resulted in a 2.2 ($p<0.001$) and 4.1 (p: 0.011) fold change increase in miR-135b expression respectively (Figure 6A&B). In absence of Wnt signaling APC binds to β-catenin and induces its ubiquitination and subsequent proteolytic degradation. Activation of Wnt signaling by binding of Wnt ligands as well as by inactivating mutations in APC binding domains causes release and stabilization of β-catenin. Stabilized β-catenin can then enter the nucleus and activate a complex transcriptional program through different effectors[22]. In order to test whether APC loss could result in miR-135b over-expression through β-catenin stabilization we enforced β-catenin expression either by transfecting NCM 4060 cells with a plasmid encoding the β-catenin protein or by stabilizing β-catenin with LiCl treatment. Both experiments resulted in increase in miR-135b expression [fold changes 3 (0.007) and 4.6 (p: 0.02) for β-catenin plasmid transfection or LiCl treatment respectively] (Figure 6C&D&E). To study which transcription factor may be responsible for miR-135b induction we used a series of siRNA against the major transcription factors involved in APC/ β-catenin axis activation. We selected two cell lines with high basal β-catenin activity: HCT-116 (β-catenin mutant[23]) or SW480 (APC mutant cells[20]). Silencing of the major transcription factors TCF4 and LEF1 resulted in miR-135b reduction in both cell models (Figure 6F&G). Interestingly, the use of siRNA against β-catenin did not alter the expression of miR-135b since in these

cells mutations in β-catenin or APC affect the β-catenin protein stability and not its transcription (Figure 6H).

Other known transcription factors (RNX3.1, USF1 and c-myc) downstream of the β-catenin axis were also screened. While RNX3.1 and c-myc did not affect miR-135b expression, USF1 silencing caused an increase in miR-135b expression suggesting that in physiological conditions USF1 might act in preventing miR-135b over-expression (Figure 6H).

Our data taken together suggest that miR-135b can be activated by the APC/β-catenin/TCF4-LEF1 pathway.

To study the pathways involved in miR-135b over-expression in the AOM/DSS model we screened miR-135b expression in a series of Mouse Embryonic Fibroblast engineered to harbor mutations in specific key genes frequently mutated in CRC. The analysis showed that miR-135b is over-expressed in PI3KCA (both subunit alpha and delta mutants) and SRC mutated cells, while mutations in c-jun did not affect miR-135b expression (Figure 7A). To further study the role of PI3K in the modulation of miR-135b we used two human CRC isogenic cell lines (HCT-116 and DLD-1) in which either the PI3K mutant or wild-type allele has been disrupted[24]. In these cell lines the PIK3CA mutations have little effect on cancer phenotype under standard conditions, but cause reduced cellular dependence on growth factors affecting cell growth and apoptosis. RT-PCR analysis showed that miR-135b expression is increased by about 2 fold in PI3K mutant compared to WT cells in basal conditions (10%FBS). Serum starvation (0.5%FBS for 19 hours) forced the PI3K mutation phenotype, resulting in a further increase in miR-135b expression (3.8 and 4.3 in HCT-116 and DLD-1 respectively) (Figure 8A&B). Serum starvation likely reduced the ability of WT cells to phosphorylate AKT, while mutant cells retained this ability in low growth factor conditions. These experiments suggest that miR-135b is dependent upon PI3K activation. The observation that miR-135b increased at a similar extent in either cell lines suggested that the activation of miR-135b is independent on whether the mutation affects the helical or the kinase domain. Further confirming these

observations we treated engineered HCT-116 cells with the PI3KCA inhibitor LY294002 after starvation and we observed that LY294002 had no effect on WT cells but reduced the expression of miR-135b by 55% in mutant cells (Figure 9A&B). We have proved so far that miR-135b expression is controlled by PI3K. The transcription factors Foxo1 and Foxo3A have been previously shown to promote the PI3K cancer associated phenotype in these engineered cell lines[24]. In order to investigate whether miR-135b is under the control of the Foxo transcription factors family we silenced Foxo1 and Foxo3A by siRNA in HCT-116 PI3K WT cells and observed an increase in miR-135b of two fold. Of note, silencing Foxo 1 and 3a in WT cells increased miR-135b to levels similar to those observed in PI3K mutant cells (Figure 9C&D). In conclusion, PI3K mutations seem to induce miR-135b by phosphorylating and inactivating Foxo1 and Foxo3A.

SRC is a member of a non membrane receptor tyrosine kinase family that act on cell proliferation, invasion and metastasis[25]. SRC can induce activation of several pathways such as MAPK/RAS/RAF, PI3K/AKT and STAT3 among others. miR-135b was found over-expressed in SRC mutated MEFs compared to WT cells (Figure 7A). Dasatinb[26], a specific SRC inhibitor, was able to reduce the expression of miR-135b in both SRC mutated MEFs and in SW620 CRC cells (Figure 10A&B&C). In the latter case the expression of miR-135b was reduced to levels observed in SW480 CRC cells. SW480 are the SW620 parental cells and show reduced SRC[27] activity compared to their metastatic derivative. Since SRC can activate a plethora of target downstream effectors we focused only on those previously analyzed in our MEF screening: PI3K and MAPK. Our data suggested that MAPK pathway is not responsible for miR-135b over-expression since mutations in c-jun which represents one of the main effectors of MAPK[28] showed no increase in miR-135b expression. Further confirming these data we used specific inhibitors of PI3K or MAPK pathway. In line with our previous findings LY294002 was able to reduce the expression of miR-135b by 40% (p:0.029) in SRC mutant MEFs while MEK1-2[29] inhibitor did not affect miR-135b expression (Figure 10D&E). These observations allowed us to speculate that, at least in part,

SRC induces miR-135b over-expression trough the PI3K/AKT/Foxo pathway. SRC affect several pathways simultaneously, thus we cannot rule out the possibility that other SRC down-stream effectors might be responsible for miR-135b over-expression. This hypothesis is supported by the observation that PI3K inhibition only in part reduces miR-135b expression and cells harboring mutations in both APC/ β-catenin and PI3K pathways still show statistically significant differences in miR-135b expression.

MiR-135b is located on the negative strand of 1q32.1 (GRCh37 1: 205417430-205417526 [-]) and overlaps with two isoforms of the LEM domain-containing 1 (LEMD1) gene (LEMD1-002 protein coding and LEMD1-005 non protein coding) (Figure 11A). LEMD1 is a cancer testis associated gene found in prostate cancer [30] and Anaplastic Cell Lymphoma[31]. Gene-expression analysis suggests that only a (657 nt) LEMD1 isoform is expressed in CRC[32]. In order to test if miR-135b is under the control of the LEMD1 promoter or under the control of an independent promoter we tested in parallel the expression of LEMD1 and miR-135b in a series of experiments in which we manipulated transcription factors involved in miR-135b expression. RT-PCR using LEMD1 primers that cover all the different spliced LEMD1 isoforms revealed no correlation between miR-135b and LEMD1 modulation suggesting that miR-135b promoter might be independent from LEMD1 promoter (Figure 11B).

MiR-135b affects apoptosis and cell growth

Our data show that miR-135b is associated with APC and PI3K mutations trough conserved mechanisms in mouse and humans. MiR-135b is associated to tumor stage and progression. In order to test if miR-135b deregulation is a consequence of cancer progression or actually drives colon carcinogenesis we tested the effect of miR-135b manipulation on apoptosis and cell growth.

APC loss is linked to reduced apoptosis in CRC cells. Indeed, re-expression of APC is able to increase apoptosis and induce cell cycle arrest in SW480 cells[33,34]. To test the contribution of miR-135b on APC mediated apoptosis, we co-

transfected SW480 cells with a plasmid encoding the full APC CDS (APC-EGFP) or an empty vector (Empty-EGFP) in combinations with LNA-anti-miR-135b, pre-miR-135b or relative scrambled oligos. In line with previous evidence, APC re-expression was able to induce apoptosis 18 hours after transfection in APC-Scrambled-LNA transfected cells (90% increase compared to Empty-EGFP-scrambled-miR transfected cells). Similarly, the inhibition of miR-135b alone induced apoptosis in SW480 cells (40% increase compared to Empty-EGFP-scrambled-miR transfected cells). The co-transfection of miR-135b and APC-EGFP was able to rescue the effect on apoptosis due to the re-induction of miR-135b (Figure 12). These data taken as a whole suggest that APC induced apoptosis is due in part by down-regulation of miR-135b. It is worth to mention that APC is a putative target of miR-135b but in our experiments the APC-EGFP vector contains only the APC CDS and not the APC 3'UTR where the miR-135b seed region is harbored. These observations suggest that the rescue effect exerted by miR-135b on APC induced apoptosis is not due to a direct interaction miR-135b-APC; it is caused instead by the effect that miR-135b exerts on other targets downstream of APC.

To test the effects of miR-135b on anchorage dependent and independent cell growth we used the HCT-116 PI3K mutant and WT cells[24]. In this isogenic cell lines the presence of activating mutations in PI3K leads to increased proliferation under stress condition (i.e. growth factor deprivation and/or serum starvation). To test whether miR-135b could affect PI3K driven cell growth we over-expressed miR-135b in PI3K WT cells and we silenced miR-135b in PI3K mutant cells (Figure 13). PI3K WT cell over-expressing miR-135b showed increased proliferation after 48 hours and the difference was still statistically significant at 5 days. Similarly, PI3K mutant cells transfected with anti-miR-135b showed reduced proliferation compared to the LNA-control cells (Figure 14A). The presence of PI3K mutations affected also the growth in soft agar. Silencing of miR-135b reduced the number of colonies in the PI3K mutant cells, while miR-135b over-expression resulted in increase colony formation. As previously shown, the total

number of colonies is not altered but only the number of colonies with a diameter grater than 2 mm[24] (Figure 14B&C).

Our findings confirmed that miR-135b has a driver role in colon carcinogenesis being responsible at least in part for the APC effect on apoptosis and the PI3K effect on cell growth.

MiR-135b targeting in vivo affect tumor number and tumor size

In order to test if miR-135b silencing can affect apoptosis and cell proliferation *in vivo* we treated AOM/DSS mice with Anti-MiR-135b oligonucleotides (miR-135b-AMO) or anti-scrambled-oligonucleotides (Scrambled-AMO). 2-MOE 3'Colesterol conjugated anti-miR-135b antisense oligodeoxyribonucleotide and scrambled probes were designed to target miR-135b or a random non-targeting sequence. We initially screened the 135b-AMO silencing efficacy in vitro in two different CRC cell lines that express high basal levels of miR-135b (HCT-116 and SW480). MiR-135b-AMO caused a 57% down-regulation in miR-135b expression in vitro after 48h, and a similar effect was still evident after 72 hours (Figure 15A). We checked for potential miR-135b-AMO off-target effects by looking at expression of other microRNAs (miR-21, miR-155, miR-221 and miR-16). None of these miRs was affected by miR-135b-AMO (Figure 15B). Bio-availability of the miR-135b-AMO was checked in vivo by injecting the oligonucleotide i.p. at 75mg/kg in 8 weeks old C57BL6 mice. Mice were euthanized 48 and 72 hours after miR-135b-AMO injection. Mice intestines and livers were collected. In order to detect miR-135b-AMO in the mouse tissues we designed an LNA oligonucleotide specific to recognize the AMO probe. In Situ Hybridization for Anti-Anti-miR-135b revealed a strong signal in colon tissues suggesting that the miR-135b-AMO probe was retained in the mice intestine. Interestingly, the signal was mainly located in the epithelial cells, while little or no signal was observed in stromal cells suggesting a selective uptake of the AMO by the epithelial compartment (Figure 15C).

In order to test miR-135b-AMO efficacy we induced colon polyps in 32 C57BL6 mice using the AOM/DSS protocol (Figure 16). Eight mice received miR-135b-

AMO i.p. twice per week at a dosage of 75mg/kg (miR-135b-AMO group), eight mice received Scrambled-AMO with the same schedule (Scrambled-AMO group), while eight mice received no AMO for the entire duration of the protocol (control group).

None of the mice showed signs of toxicity related to AMO treatment or had to be euthanized before the end of the study because of toxicity. General side effects associated to the DSS administration (weight loss, diarrhoea and rectal bleeding[11]) were observed in both arms with no difference in term of severity or number of mice affected.

After 12 weeks mice were euthanized and different organs were collected for further analyses. Mice colons were inspected during the necroscopy: tumors were counted and tumor size was measured using a calliper. The median number of tumors (tumor multiplicity) was 14.5. in the Scrambled-AMO group and 9.5 in the MiR-135b-AMO group (p: 0.016). The sum of tumor diameters (tumor load[11]) in the miR-135b-AMO group was reduced in comparison with the Scrambled-AMO group (13.9 Vs 27.5 $p<0.0001$). The difference in number of tumors with diameter grater than 2 mm was also statistically significant (3.5 in Scrambled-AMO Vs 1 in miR-135b-AMO $p<0.001$). The Average size of tumors was 2 mm and 1.5 mm in the Scrambled-AMO and miR-135b-AMO group respectively ($p<0.001$). The distribution of tumors by size also varied in the two group with increased number of tumors less than 1 mm in diameter in the miR-135b-AMO group. No differences were observed between the Scrambled-AMO and the control group (Figure 17&18A). These observations suggested that miR-135b can affect both tumor size and tumor number. Microscopic analysis of the tumors in the two groups revealed a different pattern of differentiation and architecture between the miR-135b-AMO and the scrambled-AMO group. MiR-135b-AMO tumors were well differentiated and presented an acinar pattern while tumors in the Scrambled AMO group as well as those in the control group showed low differentiation and adenomatous pattern (Figure 18B).

Real-Time PCR and ISH for miR-135b in the miR135b-AMO mice revealed that miR-135b was expressed to similar level in cancer and matched normal tissues. In Scrambled-AMO and control mice miR-135b was over-expressed in cancers compared to controls and the fold change between malignant and normal tissues were similar to those observed in the initial screening (Figure 19A&B).

Microscopic analysis suggested that miR-135b silencing might effect both proliferation and differentiation. We had previously shown miR-135b might control cell growth and apoptosis. In order to test the miR-135b-AMO effect on proliferation we performed immunohistochemistry for Ki-67 in colon tissues from miR135b-AMO, scrambled-AMO and control mice. Ki-67 scored positive in 60% of the tumors in the scrambled group while anti-miR-135b tumors had a reduced expression in the neoplastic cells. Ki67 signal was homogeneously distributed in the entire section from Scrambled-AMO mice and identified high proliferation index in different sections from different areas of the intestine (60% in Scrambled Vs 35% in the miR-135b-AMO). On the contrary Ki-67 showed a scattered pattern with differences in intensity and distribution in different areas of the intestine often reflecting different miR-135b expression (Figure 20A).

To study apoptosis we performed an Immunofluorescence based Tunel Assay. The percentage of apoptotic cells and the intensity of the signal were reduced in the anti-miR-135b tumors in comparison to the Scrambled-AMO tumors. Similarly to Ki-67 staining, the signal was not homogeneous in the same colon section or in different section leading us to hypothesize that these difference might reflect different uptake of the 135b-AMO in different areas of the mice intestine (Figure 20B).

Liver, spleen kidneys and lungs from different mice from the three treatment groups were analyzed to detect changes in morphology or miR-135b expression: no significant differences were observed found (Figure 21).

Taken together our *in vivo* data suggest that anti-miR-135b has an effect on both tumor load and tumor multiplicity. Since differentiation results from the balance between proliferation and apoptosis we suggest that differences in architecture

and differentiation might be due to the miR-135b effect on both cell growth and cell death.

miR-135b targets onco-suppressor genes involved in apoptosis, proliferation and invasion.

In order to find potential target genes affected by miR-135b over-expression we performed a gene expression in normal epithelial colon cells over-expressing miR-135b

NCM 4060 cells represents a good model for miR-135 over-expression since it is a normal colon epithelial cell line, is not affected by any mutation and shows very low basal expression of miR-135b (Figure 22). Matched analysis of a cancer associated gene panel and target prediction algorithms showed that several genes were potentially controlled by miR-135b; amongst them Factor Inhibiting HIF1a (FIH), Transforming Growth Factor β Receptor 2 (TGFβR2), and Death-associated protein kinase 1 (DAPK1) (Figure 23A). FIH is an asparagine hydroxylase that catalyzes the hydroxylation of a single conserved asparaginyl residue in the C-terminal transactivation domain of HIF-α, preventing HIF1α to exert its transcriptional activation in normoxia. TGFβR2 is a receptor transmembrane kinase involved in apoptosis and proliferation frequently down-regulated in CRC. DAPK1 is a calmodulin dependent serine-threonine kinase involved in programmed cell death.

Data from the array analysis were confirmed by RT-PCR in the same cell line and in a second normal epithelial cell line (NCM 356) after miR-135b over-expression (Figure 23&24). Using prediction algorithms we identified predicted binding sites for miR-135b in each of these gens. Luciferase experiments were performed in order to validate the prediction models. The 3'UTR of the gene of interest was sub-cloned downstream of the luciferase CDS; NCM 4060 cells were co-transfected with the luciferase construct, the pre-miR-135b or the pre-miR control and PD-TK as internal control. Over-expression of miR-135b was able to induce a

significant reduction in the expression of luciferase in the analyzed genes. Deletion of the miR-135b predicted seed region resulted in restoration of the luciferase activity confirming the specificity of the miR-135b-target interaction. Luciferase for APC was also performed in parallel and used as positive control (Figure 25).Western blotting analysis confirmed that over-expression of miR-135b induces reduction in protein expression of FIH, TGFβR2, and DAPK1 (Figure 26).

Discussion

Our findings identify miR-135b de-regulation as a consequence of mutations frequently occurring in CRC. MiR-135b over-expression is associated to increased proliferation and reduced apoptosis in vitro and recapitulates, at least in part, the phenotype associated to APC loss or PI3K activation. miR-135b silencing results in a reduction in the number and size of CRC in vivo representing a potential novel weapon strategy in CRC treatment.

MiR-135b expression data in mice tumors and in human CRC suggest that miR-135b up-regulation is an early event in tumor progression. Indeed miR-135b is increased in mouse polyps and in the sequence normal-dysplasia-cancer in the IBD associated CRC. Confirming this hypothesis we found that the two major driver events in miR-135b over-expression are represented by APC truncating mutations and PI3K activating mutations. Both mutations occur very early in the adenoma-carcinoma sequence[1,35].

Our observations are in line with a recent report that identifies miR-135b as one of the most up-regulated miR in the Inflammation-associated cancers and in the $APC^{min/+}$ mice[19]. The analogies in miR-135b expression between our model (CPC;Apc) and the $APC^{min/+}$ mice suggest that miR-135b deregulation is independent of the specific APC mutation or site of inactivation (small versus large bowel). In the same report[19], in analogy with our findings, miR-135b was not induced by inflammation alone suggesting that the synergic effect of pro-carcinogen and inflammation is crucial for the development of mutations leading to miR-135b deregulation.

The observation that miR-135b is progressively increased in more advanced CRC stages and is associated to poor prognosis suggests that other genetic aberrations might be in control of miR-135b expression. Our data suggest that SRC, a tyrosine-protein kinase frequently mutated or over-expressed in advanced and metastatic CRC might be responsible for miR-135b deregulation in advanced

stages[25]. According to our model SRC exerts its activity on miR-135 expression trough different mechanisms. PI3K is one of the SRC down-stream effectors and seems to be involved in SRC dependent miR-135b over-expression. However PI3K inhibition exerts only a partial effect in reducing miR-135b expression in SRC-MEF compared to WT-MEF suggesting that other mechanisms are in control of SRC mediated miR-135b expression. These mechanisms are probably related to pathways other than MAPK. Indeed, either over-expression of AP-1 in MEFs or MAPK inhibition in SRC modified MEFs seem no to be involved in controlling miR-135b. At the same time PI3K inhibition in SRC over-expressing cells causes on a partial decrease in miR-135b expression. We speculate that other effectors such as STAT3 might be involved in miR-135b control. This hypothesis is supported by a recent report that linked miR-135b over-expression to NPM-ALK trough STAT3 in Anaplastic Large Cell Lymphoma[31]. The same report shows that miR-135b target Foxo1; this observation lead to consider miR-135b at the center of a feedback loop in which aberrant activation of PI3K/AKT/Foxo leads to miR-135b over-expression which in turn further down -regulates Foxo1.

We identify TCF4/LEF1 as the main transcription factor complex involved the APC/β-catenin control of miR-135b regulation. However other transcription factors might be involved in the fine tuning of miR-135b regulation. Indeed USF-1 seems to play as a negative regulator of mir-135b expression. The presence of multiple transcription factors regulating miR-135b might explain why DLD-1 cells which harbor mutations in both APC and PI3K and similar SRC activity compared to HCT-116 show a significant difference in term of miR-135b basal expression. The use of animal models and MEFs characterized by different mutational background allows the dissection of specific pathways involved in microRNA control. Two important questions arise when applying these models to human CRC that display high heterogeneity. The first question relates on how different pathways crosstalk and /or act synergistically in promoting miR-135b expression. The second question is to understand whether the progressive and synchronous miR-135b up-regulation can lead to an accelerated cancer phenotype. The analysis of miR-

135b expression in human CRC cell lines suggests that miR-135b expression follows the accumulation in APC/PI3K and SRC mutations. RKO cells lack mutations in APC/β-catenin and show low basal SRC activity but have mutations in PI3K,[36-38] and are characterized by a moderate-low miR-135b expression (Figure 22). HCT-116 cells show β-catenin activating mutation[23], PI3K mutations[24,38] and moderate SRC[36] activity and present with an increased miR-135b expression compared to normal epithelium or RKO cells. Finally, parental cells SW480 and metastatic derivative SW620 show the same mutations for APC and PI3K but different SRC[38] activity and show a different pattern in miR-135b expression. The use of CRC cell lines alone allows only observational analysis while the use of consecutive rounds of gene targeting to knock-in oncogenes and knock-out multiple tumor suppressor genes may be used to generate isogenic combinatorial models that better resemble tumor plasticity. Crosstalk among different pathways is frequently observed in colon carcinogenesis; however, it seems unlikely that this might affect miR-135b expression. Since GSK3 is a key component of both APC/β-catenin and PI3K/AKT pathways, it is widely assumed that active PI3K signaling feeds positively into the Wnt pathway by protein kinase B (PKB)-mediated inhibition of GSK3. However, recent reports suggest that different pools of GSK3 kinases exist in cells, participating separately in the PI3K/PKB pathway or the Wnt/β-catenin pathway[39]. This molecular arrangement allows Wnt and PI3K inputs to have independent effects on the biological outputs of the cells that receive these signals. These observations suggest that miR-135b can be activated separately by the two axis but no feedback loops between the two systems should be involved.

Our data, in line with previously reported data suggest that APC is controlled by miR-135b[18]. Our array analysis also suggests that miR-135b can increase the transcription of β-catenin. These two observations suggest that miR-135b might be involved in a feed forward control loop. However, while miR-135b activation by the APC/β-catenin has an effect on cancer phenotype and might be of clinical relevance, the effect of miR-135b on APC/β-catenin is not completely clear. In

sporadic CRC, 80% of the tumors show somatic mutations in APC, thus in the remaining 20% miR-135b might contribute in controlling APC[35]. In IBD associated CRC, APC mutations are infrequent[40] and miR-135b which is highly expressed might have an effect on APC expression. However we must point out that while the effect of miR-135b on APC/β-catenin has been showed in vitro the effect of miR-135b on APC expression in vivo (human CRC) is not clear. IBD associated CRC show high miR-135b and often low APC signal but no nuclear β-catenin staining is observed in the same samples[40]. Agami and colleagues compared the expression levels of miR-135b in tumors with or without aberrations in the APC gene and found no association between APC mutations and miR expression[18]. We believe that the presence of multiple genomic aberrations simultaneously responsible for miR-135b over-expression might be able to explain why no correlation between miR-135b expression and mutations in APC genes have been previously reported.

miR-135b is located within the exon 1 of LEMD1. According to our experiments miR-135b and LEMD1 are associated to two different promoters since manipulation of APC or PI3K pathway can affect miR-135b expression leaving LEMD1 expression unaffected.

Matsuyama at al[31] previously reported that STAT3 can affect simultaneously miR-135b and LEMD1 expression. This discrepancy might be explained by the observation that miR function and regulation varies depending on tissue and cell specificity[5]. Furthermore five or more different LEMD1 splicing variants have been described[32], their expression varies a lot among different tissues and only one isoform seems to be expressed in CRC. The same observation might explain why PI3K seems not to be effective on miR-135b expression in Lymphoma but exerts a strong effect in CRC.

MiR-135b exerts its effect on proliferation, apoptosis and invasion by controlling different targets: TGFRβ2, DAPK1 and HIF1AN. TGFRB2 receptor levels are frequently down-regulated in both sporadic and IBD associated CRC[35]. Interestingly alteration in the expression of TGFRβ2 can affect the induction of

apoptosis by TGF beta by modulating SMAD dependent and independent pathways[41,42]. Similarly DAPK1 is frequently found down-regulated in both AOM CRC model and human CRC[43,44]. Interestingly, while DAPK1 is frequently silenced by methylation in hematological and some solid malignancies, DAPK1 promoter methylation is infrequent in CRC[43,44].

MicroRNA based therapeutics represent a promising tool for targeted cancer treatment since the same microRNA can regulate several survival-signaling pathways[9]. This observation summarizes promises and potential pitfalls of miR based therapeutics. If a single miR can affect several oncogenic pathways, it might also affect several cell homeostasis pathways crucial for cell physiology. MiR-21 for example can be considered a major onco-miR but is also central in cardiovascular physiology[9]. Thus selection of the right target is a central issue to avoid massive off-target effects. Contrary to miR-21, miR-135b basal expression is very low in normal epithelium as well as other organs suggesting that silencing miR-135b in normal intestine might have little or no effect on intestinal physiology. Anti-miR technology shows more potential than miR replacement technology. Even though miRs are smaller and less antigenic than protein-coding genes, miR delivery still represent an issue since viral-based delivery mechanisms are hardly translatable into clinical practice[9]. On the contrary miR silencing by specific antagomiRs or small sponges that soak-up a broader spectrum of miRNAs, can be efficiently achieved with an *in vivo* effect that can be sustained from few days up to 3 weeks[9]. Systemically delivered antagomirs have been successfully employed in liver and metastatic cancer models and are currently undergoing clinical trial testing[45,46]. Beside bioavailability and toxicities related to miR conjugation that might be in some way common to anti-miR and miR replacement therapies, anti-miR technology offers a major advantage over miR replacement: miRNA over-expression could cause saturation of the miRNA machinery and non-specific effects. For example, Exportin 5 and Argonaute 2, two key miRNA processing components, are down-regulated when miRNA levels are too elevated[47,48]. A second example is represented by DICER that is an

haploinsufficient tumour suppressor gene. Uncontrolled miR over-expression may repress DICER function and cause a tumour-prone environment[49]. All these issues are not associated to anti-miR technology where a single miR is silenced and not over-expressed. In conclusion, even tough pre-clinical studies like this report represent a good proof of principle they will need clinical trial evaluation to address several question associated to efficacy, toxicity and off target effects.

Materials and Methods

MicroRNA and mRNA expression analysis

MicroRNA expression profiling and mRNA expression of cancer associated genes were analyzed using Nanostring nCounter Technology (Seattle WA0 using the nCounter Mouse miRNA Expression Assay Kit and the nCounter Human Cancer Reference Kit respectively. NanoString nCounter gene expression system quantitates abundances of miRNAs and mRNA. Technical normalization was performed using the synthetic positive controls to adjust the counts for each miRNA/mRNA target in that assay. Then biological normalization is performed to correct for differences in sample abundances. Each sample is normalized to the geometric mean of the top 50 most highly expressed miRNAs/mRNA. Students t-test is used on normalized counts to calculate statistical significances of pair-wise comparisons . All of the calculations are performed in R statistical computing and graphics environment (http://www.r-project.org).

Cell Cultures and Transfections

SW620, SW480, HCT-116, DLD-1 and RKO colorectal cancer (CRC) cells (American Type Culture Collection ATCC Manassas, VA) were cultured in RPMI 1640 (Gibco, Carlsbad, CA). PI3KCA mutant and WT HCT-116 and DLD-1 cells (kind gift Prof Bert Vogelstein Johns Hopkins University Baltimore MD USA)) were grown in McCoy's 5A modified medium (Gibco, Carlsbad, CA). All cells were supplemented with 10% fetal bovine serum (Sigma, St. Louis, MO) plus antibiotics. For serum starvation, cells were grown to 70%–80% confluency, washed once with PBS, and incubated for 19 hr in McCoy's 5A modified medium containing 0.5% FCS. Normal epithelial colon cell lines NCM356 and NCM4060 (InCell San Antonio, TX) were cultured in M3:10TM medium. Mouse Embryo Fibroblasts were provided by Prof. Peter K Vogt (Scripps Research Institute La Jolla CA USA) and cultured in 10% DMEM plus antibiotics. Cells were examined

for Mycoplasma contamination periodically and were always found negative. Cell transfections were performed using Lipofectamine 2000 (Invitrogen, Carlsbad, CA) following manufacturer's protocol. For over-expression studies specific miRNA or control precursor oligonucleotides were purchased from Ambion (Austin, TX) and used at 20 nM. On target-plus siRNA pools and relative controls were purchased from Thermo Fisher Scientific (Lafayette, CO). For silencing experiments miRCURY LNA™ anti-miR-135b or control miRCURY knockdown probes (Exiqon, Vedbaek, Denmark) were used at 25 nM. EGFP-APC and empty control vectors were a gift from Prof Joanna Groden (OSU OH USA). The PI3K inhibitor LY294002 was purchased at Cell Signaling (Beverly MA) and used as described previously at 10 μM. Dasatinb (Selleck Chemicals Houston, TX) was used as previously described at 100nmol/L. AS703026 a MEK1-2 inhibitor (Selleck Chemicals Houston, TX) was used as previously described at 10 μmol/L

Luciferase Assay

The predicted miRNA binding sites in the 3'-UTR of FIH, TGFβR2 and APC were cloned downstream of the firefly luciferase gene as follows. Complimentary DNA (cDNA) from NCM4060 cells was amplified by PCR using specific primers (primers sequences available upon request). The product was then digested with SpeI and SacII (New England Biolabs Ipswich, MA) and inserted into the pGL3 control vector (Promega, Madison, WI) previously modified to harbor the SpeI and SacII sites immediately downstream of the stop codon of the firefly luciferase gene. The DAPK1-3'UTR plasmid was purchased at SwitchGear Genomics (Menlo Park, CA) and transfected as previously described[50]. Mutant plasmids harboring a deletion in the miR-135b seed region were prepared, for each target gene, using QuikChange site-directed mutagenesis kit (Stratagene, San Diego, CA). NCM 4060 cells were co-transfected in 12-well plates with 1 μg of pGL3 firefly luciferase reporter control vector, 0.1 μg of the phRL-SV40 control vector (Promega, Madison, WI), and 20 nM pre-miR-135b or control precursors. Firefly

and Renilla luciferase activities were measured consecutively by using the Dual Luciferase Assay (Promega) 24 hours after transfection.

Western Blotting

For immunoblotting analysis cells were lysed with ice-cold Cell Lysis Buffer plus protease inhibitor (Cell Signaling Technology Inc. Danvers, MA). Equivalent amounts of protein were resolved and mixed with 4X SDS-PAGE sample buffer, electrophoresed in a 4%–20% and 7.5% linear gradient Tris-HCL Criterion Precast Gels (Bio-Rad), and transferred to nitrocellulose or PVDF membranes (Bio-Rad). The membranes were blocked with 5% nonfat dry milk in Tris-buffered saline, pH 7.4, containing 0.05% Tween 20, and were incubated with primary and secondary antibodies according to the manufacturer's instructions. The following Antibodies were used: Phospho-Akt Pathway Sampler Kit (Cell Signaling cat n 9916); Anti-DAP Kinase 1 rabbit (Sigma cat n D1319); Phospho-p44/42 MAPK (Erk1/2) (Thr202/Tyr204) (Cell Signaling cat n 9101S); p44/42 MAPK (Erk1/2) (Cell Signaling cat n 9102); FIH (Cell Signaling cat n D19B3); β-Catenin (Cell Signaling cat n #9562); p21 Waf1/Cip1 (12D1) Rabbit (Cell Signaling cat n #2947); TGF-β Receptor II (K105) (Cell Signaling cat n #3713) GAPDH (St Cruz CA)

Real time PCR for mature miRNAs and genes

Total RNA was isolated using Trizol (Invitrogen). Mature miRNAs expression was assessed by single-tube TaqMan MicroRNA Assay, while the expression of mRNAs of interest was evaluated by the Gene Expression analysis using Syber-Green or Taq-man Probes. For Syber-Green, RNA was treated with RNase-free DNase I (Qiagen). One microgram of RNAwas reverse-transcribed to cDNA, and quantitative real-time PCR was performed with specific primers for IL8, VEGF, DAPK1, FIH, APC and TGFβR2 (list of primers available upon request). TaqMan Probes were as follow: TGFBR2 (Hs00234253_m1), HIF1AN (Hs00215495_m1), DAPK1 (Hs00234489_m1). miRNA expression was normalized to that of RNU44

and RNU48. Gene expression was normalized to GAPDH. All retrotranscriptase (RT) reactions, including no-template controls and RT minus controls, were run in a GeneAmp PCR 9700 Thermocycler (Applied Biosystems). Each sample was tested in triplicate.

Cell Death analysis

Propidium iodide (PI) staining: cells were detached with trypsin, washed with cold phosphate-buffered saline (PBS)–5% FCS and then fixed in 70% ethanol for 24 h. After washing with PBS, cells were incubated with 1 μg/ml PI for 3 h at 25°C before FACS analysis by Coulter Epics XL flow cytometer (Beckman Coulter, Fullerton, CA). Cells were considered apoptotic when their DNA content was <2N. For detection of caspase-3/7 activity, cells were plated in 10cm dishes transfected with pre-miR-135b, siRNA to p21 or TGFβR2. The day after transfection cells were harvested and re-plated in 96-well plates in quadruplicate, treated with 10 μM TGF and analyzed using a Caspase-Glo 3/7 Assay kit (Promega) according to the manufacturer's instructions.

Focus formation assay in soft agar

HCT116 transfected with pre-miR-135b, LNA anti-miR-135b or relative contols were plated in triplicate at 5000 cells/ml in top plugs consisting of McCoy's 5A modified medium containing various FCS concentrations and 0.4% SeaPlaque agarose (FMC Bioproducts, Rockland, Maine). After two weeks, the colonies were photographed and counted. When all colony sizes were considered, the total number of colonies formed by WT and mutant clones was essentially the same. However, when colonies above the threshold of 2 mm were counted, differences between the number of WT and mutant clones were observed.

Cell viability assays.Cell viability was examined with 3-(4,5-dimethylthiazol-2-yl)-2,5-diphenyltetrazolium bromide (MTS)-Cell Titer 96 Aqueous One Solution Cell

Proliferation Assay (Promega) according to the manufacturer's protocol. Metabolically active cells were detected by adding 20 µl of MTS to each well. After 1 h of incubation, the plates were analyzed in a Multilabel Counter (Bio-Rad Laboratories).

Tube Formation Assay NCM 4060 cells were transfected with pre-miR-135b or pre-miR-control under starvation. 16 hours after transfection media from both experiments was collected and used to culture HUVEC Matrigel (BD PharMingen; 12.9 mg/mL)–coated LabTek (55,000 cells per chamber). Results are expressed as number of tube-like structures per field (magnification, ×200).

Tissue Collection

Fresh frozen tissues from tumor and normal adjacent tissue from 62 cases of CRC were collected at the Istituto Scientifico Romagnolo per lo Studio e la Cura dei Tumori, Meldola, Italy after approval of the ethical committee. Cell lysates for protein and RNA extraction were extracted previousy described. Nine cases of Inflammatory Bowel Disease (IBD) associated CRC and matched normal tissues were collected at the OSU Pathology Archive. Six cases of IBD associated CRC were collected at the Department of Pathology at the University of Ferrara Italy. In four of these cases high grade dysplasia was also availbale.

Animals and Tumor Induction

RNAs from $Apc^{+/\Delta 716}$ $Cdx2^{+/-}$ (matched cancer and normal), Azoximehtane (AOM)/Dextran Sulphate Sodium (DSS) (matched cancer and normal), Wild Type (untreated normal epithelium) and short term DSS treated mice (inflamed epithelium) for the initial microRNA expression screening were provided by Prof Michael Karin (UCSD USA). RNA from long term (78 days) DSS treated mice (inflamed epithelium) was collected at OSU. All mice were C75BL/6 strain mice. For in vivo silencing experiments C57BL/6 mice were obtained from The Jackson Laboratory. All mice were maintained in filter-topped cages on autoclaved food and water at OSU according to NIH guidelines, and all experiments were

performed in accordance with OSU and NIH guidelines and regulations. CAC was induced as described previously. Briefly, on day 1, mice were injected intra-peritoneally (i.p.) with 12.5 mg/kg azoxymethane (AOM; National Cancer Institute) and maintained on regular diet and water for 7 days. After 7 days, mice received water with 2.5% dextran sulfate sodium (DSS; MP Biomedicals, molecular weight 35,000–50,000 kDa) for 5 days. After this, mice were maintained on regular water for 14 days and subjected to two more DSS treatment cycles.

Mice were treated as follows:

AOM + DSS + Scrambled-AMO (Scrambled-AMO group) (n=8) C57BL/6 8 weeks old mice were treated with AOM i.p. at day 0 and received 2.5% DSS water accordingly to the above mentioned schedule. Anti-miR-control was given twice a week for the entire treatment (22 injections over a 11 weeks period) at 75mg/kg.

AOM + DSS + miR-135b-AMO (135b-AMO treatment group) (n=8) C57BL/6 8 weeks old mice were treated with AOM i.p. at day 0 and received 2.5% DSS water accordingly to the above mentioned schedule. Anti-miR-135b was given twice a week for the entire treatment (22 injections over a 11 weeks period) at 75mg/kg.

AOM + DSS (Mock Group) (n=8) C57BL/6 8 weeks old mice were treated with AOM i.p. at day 0 and will receive 3% DSS water accordingly to the above mentioned schedule. No anti-miRs were administered.

Macroscopic tumors were counted and measured with a caliper. Tumors and matched normal adjacent tissues from the distal colon were taken as a tissue sample and snap frozen in liquid nitrogen, maintained in Trizol or fixed in 10% neutral buffered formalin for 24 hr and transferred to 70% ethanol for subsequent paraffin embedding and histological analysis. The clinical course of disease was followed daily by measurement of body weight and monitoring for signs of rectal bleeding or diarrhoea.

Histological Analysis

Colons were examined using 4 μm thick, 200 μm step serial sections stained with hematoxylin and eosin. For TUNEL assay, an In Situ Cell Death Kit (Roche) was used according to the manufacturer's recommendations. MicroRNA detection was performed on colon cancer tissues from mice intestines or human colon cancer sections by in situ hybridization (ISH) as previously described[51]. The negative controls included omission of the probe and the use of a scrambled LNA probe. Immunohistochemistry for Ki-67 was performed as previously described at the OSU core pathology facility.

Statistical Analysis

Expression graphs and Wilcoxon matched-pairs tests were used to analyze differences in microRNA expression between tumors and paired nontumorous tissue for all quantitative RT-PCR data using Graphpad Prism 5.0 (Graphpad Software Inc, San Diego, California). Associations with prognosis in the sporadic CRC cohort were considered statistically significant only if the P value were less than .01 to adjust for multiple comparisons testing (5 tests using a Bonferroni correction). KaplanMeier analysis was performed with WINSTAT 2001 (R Fitch Software, Bad Krozingen, Germany). Multivariate Cox regression analysis was performed using StataCorp 9.2. For these models, we dichotomized age as 50 years or older vs younger than 50 years because the recommended screening age for colon cancer is at age 50 years; TNM staging was dichotomized based on metastasic vs nonmetastasic disease. Univariate Cox regression was performed on each clinical covariate to examine influence of each on patient survival. Final multivariate models were based on stepwise addition and removal of clinical covariates found to be associated with poor survival in univariate models ($P < .10$). A Wald statistic of $P < .05$ was used as the criterion for inclusion in final multivariate models. All stepwise addition models gave the same final models as stepwise removal models. All P values reported are 2-sided. All univariate and

multivariate Cox regression models were tested for proportional hazards assumptions based on Schoenfeld residuals, and no model violated these assumptions. Results of statistical analyses are expressed as mean ± SD unless indicated otherwise. Comparisons between groups were performed using the two-tailed Student's t test. A P value <0.05 was considered significant. Graphpad Prism version 5.0 was used for Pearson correlations.

Reference List

1. Sjöblom T, Jones S, Wood LD, Parsons DW, Lin J, Barber TD, Mandelker D, Leary RJ, Ptak J, Silliman N, Szabo S, Buckhaults P, Farrell C, Meeh P, Markowitz SD, Willis J, Dawson D, Willson JK, Gazdar AF, Hartigan J, Wu L, Liu C, Parmigiani G, Park BH, Bachman KE, Papadopoulos N, Vogelstein B, Kinzler KW, Velculescu VE. The consensus coding sequences of human breast and colorectal cancers. Science. 2006 Oct 13;314(5797):268-74.
2. De Roock W, De Vriendt V, Normanno N, Ciardiello F, Tejpar S. KRAS, BRAF, PIK3CA, and PTEN mutations: implications for targeted therapies in metastatic colorectal cancer. Lancet Oncol. 2011 Jun;12(6):594-603.
3. Catenacci DV, Kozloff M, Kindler HL, Polite B. Personalized colon cancer care in 2010. Semin Oncol. 2011 Apr;38(2):284-308.
4. Prahallad A, Sun C, Huang S, Di Nicolantonio F, Salazar R, Zecchin D, Beijersbergen RL, Bardelli A, Bernards R. Unresponsiveness of colon cancer to BRAF(V600E) inhibition through feedback activation of EGFR. Nature. 2012 Jan 26.
5. Croce CM. Causes and consequences of microRNA dysregulation in cancer. Nat. Rev. Genet. 2009 10, 704-714
6. Valeri N, Croce CM, Fabbri M. Pathogenetic and clinical relevance of microRNAs in colorectal cancer. Cancer Genomics Proteomics. 2009 Jul-Aug;6(4):195-204.
7. Ichimura A, Ruike Y, Terasawa K, Tsujimoto G. miRNAs and regulation of cell signaling. FEBS J. 2011 May;278(10):1610-8
8. Wasik KA, Rebbeck CA. Keystone symposia 40th season: microRNAs and noncoding RNAs in cancer. Cancer Res. 2011 Oct 1;71(19):6102-5.
9. Kasinski AL, Slack FJ. Epigenetics and genetics. MicroRNAs en route to the clinic: progress in validating and targeting microRNAs for cancer therapy. Nat Rev Cancer. 2011 Nov 24;11(12):849-64.

10. Hinoi T, Akyol A, Theisen BK, Ferguson DO, Greenson JK, Williams BO, Cho KR, Fearon ER Mouse model of colonic adenoma-carcinoma progression based on somatic Apc inactivation. Cancer Res. 2007 Oct 15;67(20):9721-30.

11. Grivennikov S, Karin E, Terzic J, Mucida D, Yu GY, Vallabhapurapu S, Scheller J, Rose-John S, Cheroutre H, Eckmann L, Karin M. IL-6 and Stat3 are required for survival of intestinal epithelial cells and development of colitis-associated cancer. Cancer Cell. 2009 Feb 3;15(2):103-13.

12. Chen J, Huang XF. The signal pathways in azoxymethane-induced colon cancer and preventive implications. Cancer Biol Ther. 2009 Jul;8(14):1313-7.

13. Kohno H, Suzuki R, Sugie S, Tanaka T. Beta-Catenin mutations in a mouse model of inflammation-related colon carcinogenesis induced by 1,2-dimethylhydrazine and dextran sodium sulfate. Cancer Sci. 2005 Feb;96(2):69-76.

14. Ng EK, Chong WW, Jin H, Lam EK, Shin VY, Yu J, Poon TC, Ng SS, Sung JJ. Differential expression of microRNAs in plasma of patients with colorectal cancer: a potential marker for colorectal cancer screening. Gut. 2009 Oct;58(10):1375-81.

15. Bandrés E, Cubedo E, Agirre X, Malumbres R, Zárate R, Ramirez N, Abajo A, Navarro A, Moreno I, Monzó M, García-Foncillas J. Identification by Real-time PCR of 13 mature microRNAs differentially expressed in colorectal cancer and non-tumoral tissues. Mol Cancer. 2006 Jul 19;5:29.

16. Slattery ML, Wolff E, Hoffman MD, Pellatt DF, Milash B, Wolff RK. MicroRNAs and colon and rectal cancer: differential expression by tumor location and subtype. Genes Chromosomes Cancer. 2011 Mar;50(3):196-206. doi: 10.1002/gcc.20844.

17. Oberg AL, French AJ, Sarver AL, Subramanian S, Morlan BW, Riska SM, Borralho PM, Cunningham JM, Boardman LA, Wang L, Smyrk TC, Asmann Y, Steer CJ, Thibodeau SN. miRNA expression in colon polyps provides evidence for a multihit model of colon cancer. PLoS One. 2011;6(6)

18. Nagel R, le Sage C, Diosdado B, van der Waal M, Oude Vrielink JA, Bolijn A, Meijer GA, Agami R. Regulation of the adenomatous polyposis coli gene by the miR-135 family in colorectal cancer. Cancer Res. 2008 Jul 15;68(14):5795-802.

19. Necela BM, Carr JM, Asmann YW, Thompson EA. Differential expression of microRNAs in tumors from chronically inflamed or genetic (APC(Min/+)) models of colon cancer. PLoS One. 2011 Apr 12;6(4)

20. Qian J, Sarnaik AA, Bonney TM, Keirsey J, Combs KA, Steigerwald K, Acharya S, Behbehani GK, Barton MC, Lowy AM, Groden J. The APC tumor suppressor inhibits DNA replication by directly binding to DNA via its carboxyl terminus. Gastroenterology. 2008 Jul;135(1):152-62

21. Moyer MP, Stauffer JS, Manzano LA, Tanzer LR, Merriman RL. NCM460, A Normal Human Colon Mucosal Epithelial Cell Line. In Vitro Cell Dev Biol: Animal 32:315-317, 1996.

22. Myant K, Sansom OJ. Wnt/Myc interactions in intestinal cancer: partners in crime. Exp Cell Res. 2011 Nov 15;317(19):2725-31.

23. Ilyas M, Tomlinson IP, Rowan A, Pignatelli M, Bodmer WF. Beta-catenin mutations in cell lines established from human colorectal cancers. Proc Natl Acad Sci U S A. 1997 Sep 16;94(19):10330-4.

24. Samuels Y, Diaz LA Jr, Schmidt-Kittler O, Cummins JM, Delong L, Cheong I, Rago C, Huso DL, Lengauer C, Kinzler KW, Vogelstein B, Velculescu VE. Mutant PIK3CA promotes cell growth and invasion of human cancer cells. Cancer Cell. 2005 Jun;7(6):561-73.

25. Yeatman TJ. A renaissance for SRC. Nat Rev Cancer. 2004 Jun;4(6):470-80.

26. Serrels A, Macpherson IR, Evans TR, Lee FY, Clark EA, Sansom OJ, Ashton GH, Frame MC, Brunton VG. Identification of potential biomarkers for measuring inhibition of Src kinase activity in colon cancer cells following treatment with dasatinib. Mol Cancer Ther. 2006 Dec;5(12):3014-22.

27. Baker AM, Cox TR, Bird D, Lang G, Murray GI, Sun XF, Southall SM, Wilson JR, Erler JT. The role of lysyl oxidase in SRC-dependent proliferation and metastasis of colorectal cancer. J Natl Cancer Inst. 2011 Mar 2;103(5):407-24.

28. Shaulian E. AP-1--The Jun proteins: Oncogenes or tumor suppressors in disguise? Cell Signal. 2010 Jun;22(6):894-9.

29. Yoon J, Koo KH, Choi KY. MEK1/2 inhibitors AS703026 and AZD6244 may be potential therapies for KRAS mutated colorectal cancer that is resistant to EGFR monoclonal antibody therapy. Cancer Res. 2011 Jan 15;71(2):445-53.

30. Ghafouri-Fard S, Ousati Ashtiani Z, Sabah Golian B, Hasheminasab SM, Modarressi MH. Expression of two testis-specific genes, SPATA19 and LEMD1, in prostate cancer. Arch Med Res. 2010 Apr;41(3):195-200.

31. Matsuyama H, Suzuki HI, Nishimori H, Noguchi M, Yao T, Komatsu N, Mano H, Sugimoto K, Miyazono K. miR-135b mediates NPM-ALK-driven oncogenicity and renders IL-17-producing immunophenotype to anaplastic large cell lymphoma. Blood. 2011 Dec 22;118(26):6881-92.

32. Yuki D, Lin YM, Fujii Y, Nakamura Y, Furukawa Y. Isolation of LEM domain-containing 1, a novel testis-specific gene expressed in colorectal cancers. Oncol Rep. 2004 Aug;12(2):275-80.

33. Morin PJ, Vogelstein B, Kinzler KW. Apoptosis and APC in colorectal tumorigenesis. Proc Natl Acad Sci U S A. 1996 Jul 23;93(15):7950-4.

34. Groden J, Joslyn G, Samowitz W, Jones D, Bhattacharyya N, Spirio L, Thliveris Robertson M, Egan S, Meuth M, et al. Response of colon cancer cell lines to the introduction of APC, a colon-specific tumor suppressor gene. Cancer Res. 1995 Apr 1;55(7):1531-9.

35. Markowitz SD, Bertagnolli MM. Molecular origins of cancer: Molecular basis of colorectal cancer. N Engl J Med. 2009 Dec 17;361(25):2449-60.

36. Dehm S, Senger MA, Bonham K. SRC transcriptional activation in a subset of human colon cancer cell lines. FEBS Lett. 2001 Jan 5;487(3):367-71.

37. da Costa LT, He TC, Yu J, Sparks AB, Morin PJ, Polyak K, Laken S, Vogelstein B, Kinzler KW. CDX2 is mutated in a colorectal cancer with normal APC/beta-catenin signaling. Oncogene. 1999 Sep 2;18(35):5010-4.

38. Abubaker J, Bavi P, Al-Harbi S, Ibrahim M, Siraj AK, Al-Sanea N, Abduljabbar A, Ashari LH, Alhomoud S, Al-Dayel F, Uddin S, Al-Kuraya KS. Clinicopathological analysis of colorectal cancers with PIK3CA mutations in Middle Eastern population. Oncogene. 2008 Jun 5;27(25):3539-45.

39. Ng SS, Mahmoudi T, Danenberg E, Bejaoui I, de Lau W, Korswagen HC, Schutte M, Clevers H. Phosphatidylinositol 3-kinase signaling does not activate the wnt cascade. J Biol Chem. 2009 Dec 18;284(51):35308-13.

40. Leedham SJ, Graham TA, Oukrif D, McDonald SA, Rodriguez-Justo M, Harrison RF, Shepherd NA, Novelli MR, Jankowski JA, Wright NA. Clonality, founder mutations, and field cancerization in human ulcerative colitis-associated neoplasia. Gastroenterology. 2009 Feb;136(2):542-50.

41. Biswas S, Chytil A, Washington K, Romero-Gallo J, Gorska AE, Wirth PS, Gautam S, Moses HL, Grady WM. Transforming growth factor beta receptor type II inactivation promotes the establishment and progression of colon cancer. Cancer Res. 2004 Jul 15;64(14):4687-92.

42. Guda K, Giardina C, Nambiar P, Cui H, Rosenberg DW. Aberrant transforming growth factor-beta signaling in azoxymethane-induced mouse colon tumors. Mol Carcinog. 2001 Aug;31(4):204-13.

43. Borinstein SC, Conerly M, Dzieciatkowski S, Biswas S, Washington MK, Trobridge P, Henikoff S, Grady WM. Aberrant DNA methylation occurs in colon neoplasms arising in the azoxymethane colon cancer model. Mol Carcinog. 2010 Jan;49(1):94-103.

44. Xu XL, Yu J, Zhang HY, Sun MH, Gu J, Du X, Shi DR, Wang P, Yang ZH, Zhu JD. Methylation profile of the promoter CpG islands of 31 genes that may contribute to colorectal carcinogenesis. World J Gastroenterol. 2004 Dec 1;10(23):3441-54.

45. Lanford RE, Hildebrandt-Eriksen ES, Petri A, Persson R, Lindow M, Munk ME, Kauppinen S, Ørum H. Therapeutic silencing of microRNA-122 in primates with chronic hepatitis C virus infection. Science. 2010 Jan 8;327(5962):198-201.

46. Ma L, Reinhardt F, Pan E, Soutschek J, Bhat B, Marcusson EG, Teruya-Feldstein J, Bell GW, Weinberg RA. Therapeutic silencing of miR-10b inhibits metastasis in a mouse mammary tumor model. Nat Biotechnol. 2010 Apr;28(4):341-7.

47. Grimm D, Streetz KL, Jopling CL, Storm TA, Pandey K, Davis CR, Marion P, Salazar F, Kay MA. Fatality in mice due to oversaturation of cellular microRNA/short hairpin RNA pathways. Nature. 2006 May 25;441(7092):537-41.

48. Grimm D, Wang L, Lee JS, Schürmann N, Gu S, Börner K, Storm TA, Kay MA. Argonaute proteins are key determinants of RNAi efficacy, toxicity, and persistence in the adult mouse liver. J Clin Invest. 2010 Sep;120(9):3106-19.

49. Kumar MS, Pester RE, Chen CY, Lane K, Chin C, Lu J, Kirsch DG, Golub TR, Jacks T. Dicer1 functions as a haploinsufficient tumor suppressor. Genes Dev. 2009 Dec 1;23(23):2700-4.

50. Iliopoulos D, Rotem A, Struhl K. Inhibition of miR-193a expression by Max and RXRα activates K-Ras and PLAU to mediate distinct aspects of cellular transformation. Cancer Res. 2011 Aug 1;71(15):5144-53.

51. Nuovo GJ. In situ detection of microRNAs in paraffin embedded, formalin fixed tissues and the co-localization of their putative targets. Methods. 2010 Aug 17.

Figures

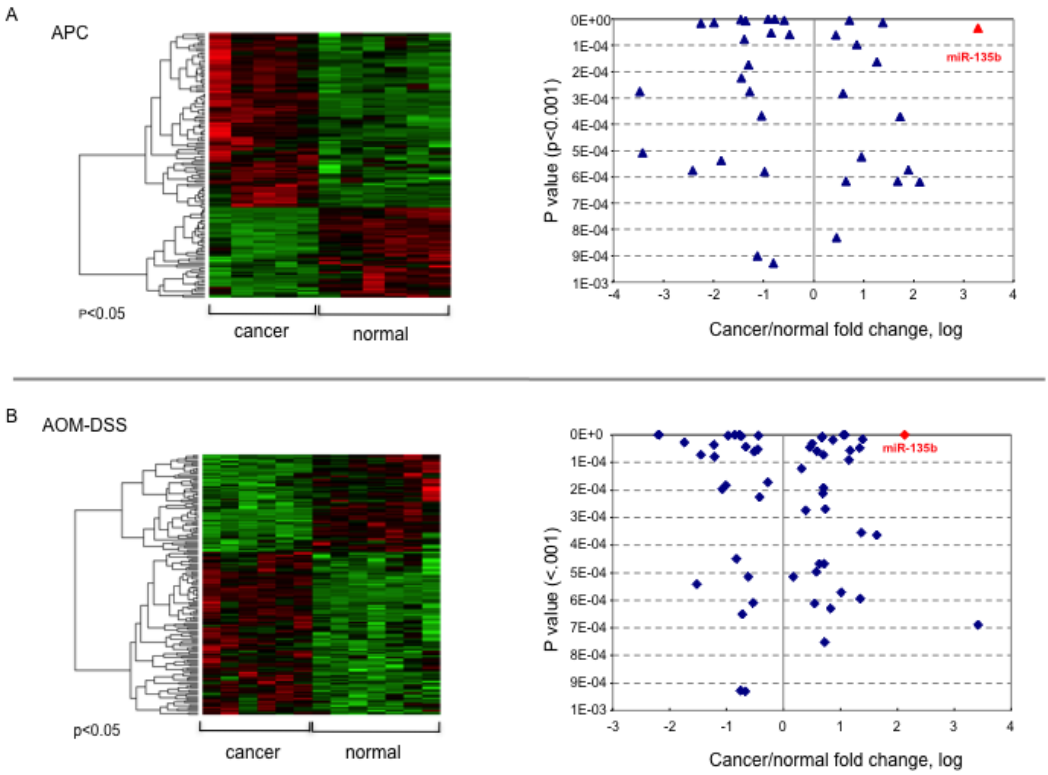

Figure 1. A. Genome-wide expression miRNA profiling was performed in colon tissue from APC vs WT mice. On the right panel the ratio of expression of selected miRNAs (p<0.001) in cancer relative to normal tissue is plotted against the *p*-value. **B.** Same analysis as above in mice treated with AOM-DSS to study inflammation-induced CRC.

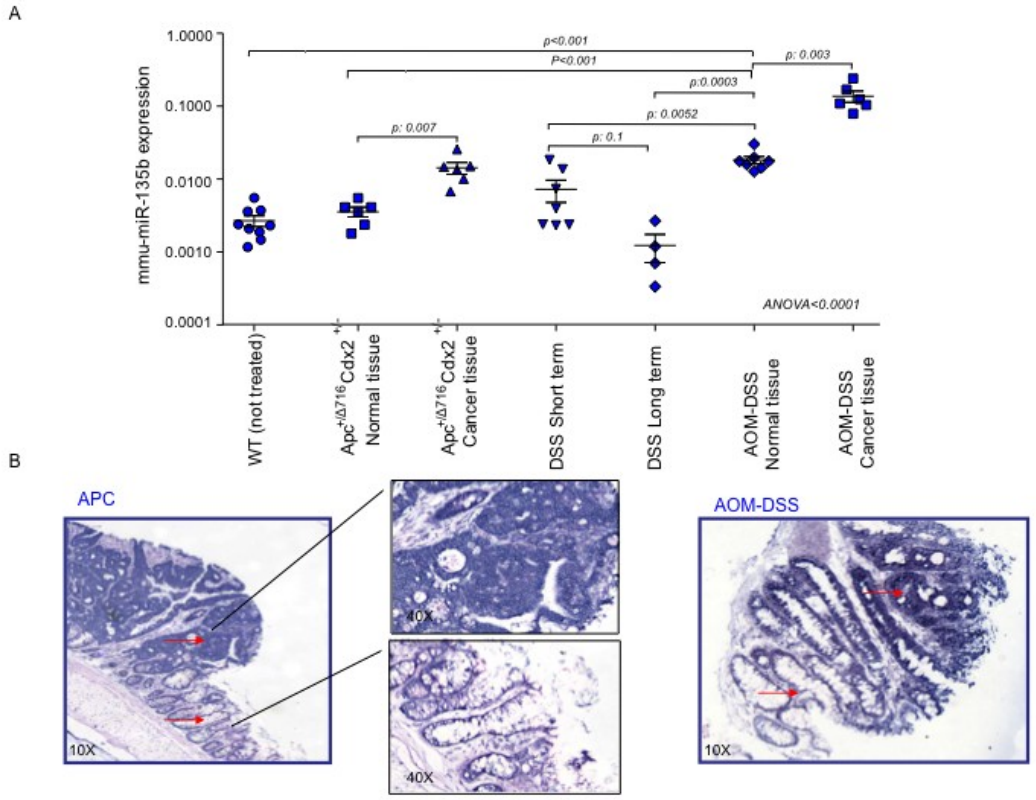

Figure 2. A. miR-135b expression was assessed by real time PCR in mouse tissues. The expression of miR-135b was normalized to that of RNU135. Bars represent mean and SEM of 3 samples. Significant comparisons are annotated. **B.** Paraffin-embedded, formalin-fixed colon tissues were incubated with LNA-anti-miR-135b.

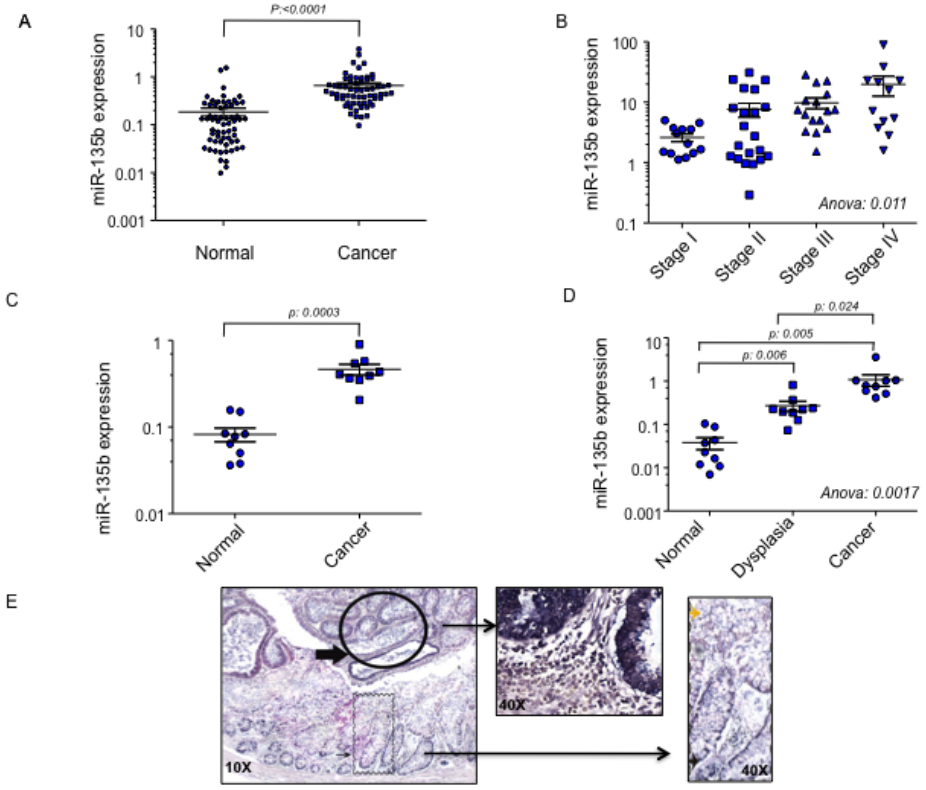

Figure 3. hsa-miR-135b expression was assessed by real time PCR in human tissues. The expression of miR-135b was normalized to that of RNU48. **A.** Expression of hsa-miR-135b in sporadic CRCs. Bars represent the mean and SD. **B.** hsa-miR-135b expression in sporadic CRCs by stages. **C.** hsa-miR-135b expression in an American cohort of IBD-associated CRCs. **D.** hsa-miR-135b expression in an Italian cohort of IBD-associated CRCs. **E.** Paraffin-embedded, formalin-fixed sporadic CRC tissue was incubated with LNA-anti-miR-135b.

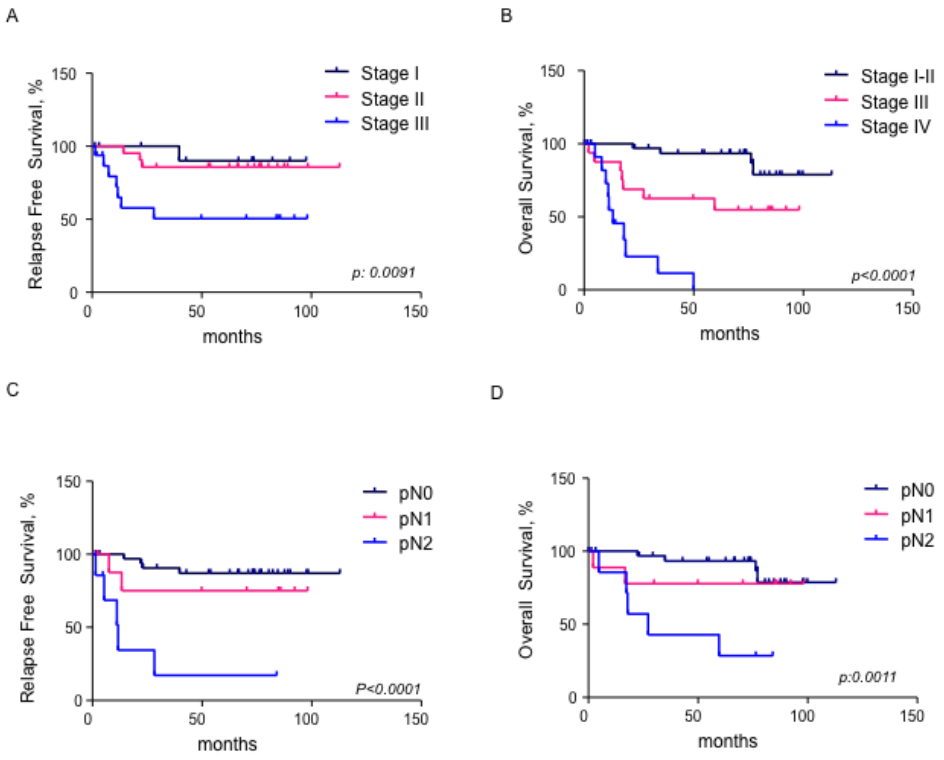

Figure 4. miR-135b expression was assessed by real time PCR in human tissues from sporadic CRCs. The expression of miR-135b was normalized to that of RNU48 and expressed in log2 scale. The ratio between the expression of mi<r-135b in cancer and normal was divided in: Low miR-135b ≤2, while high mR-135b >2. Kaplan Meyer analysis was performed in all stages (**A**), stages I to III (**B**), stages II and III (**C**), and stage II (**D**).

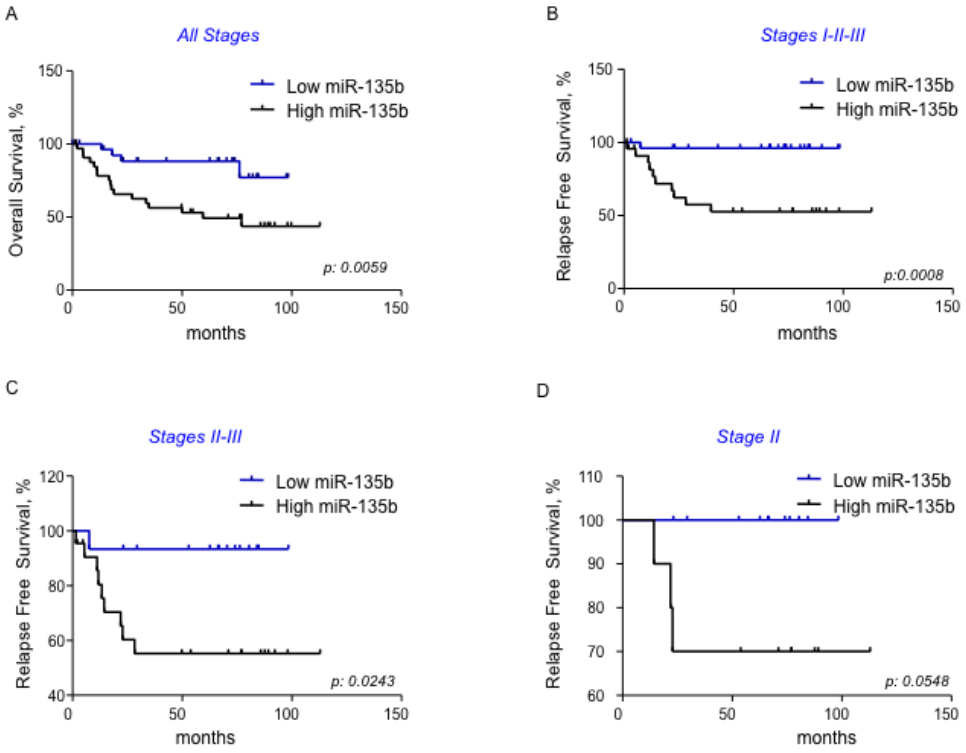

Figure 5. Relapse and Overall Survival was analyzed by Kaplan Meyer analysis in sporadic CRCs according to stage and nodal status.

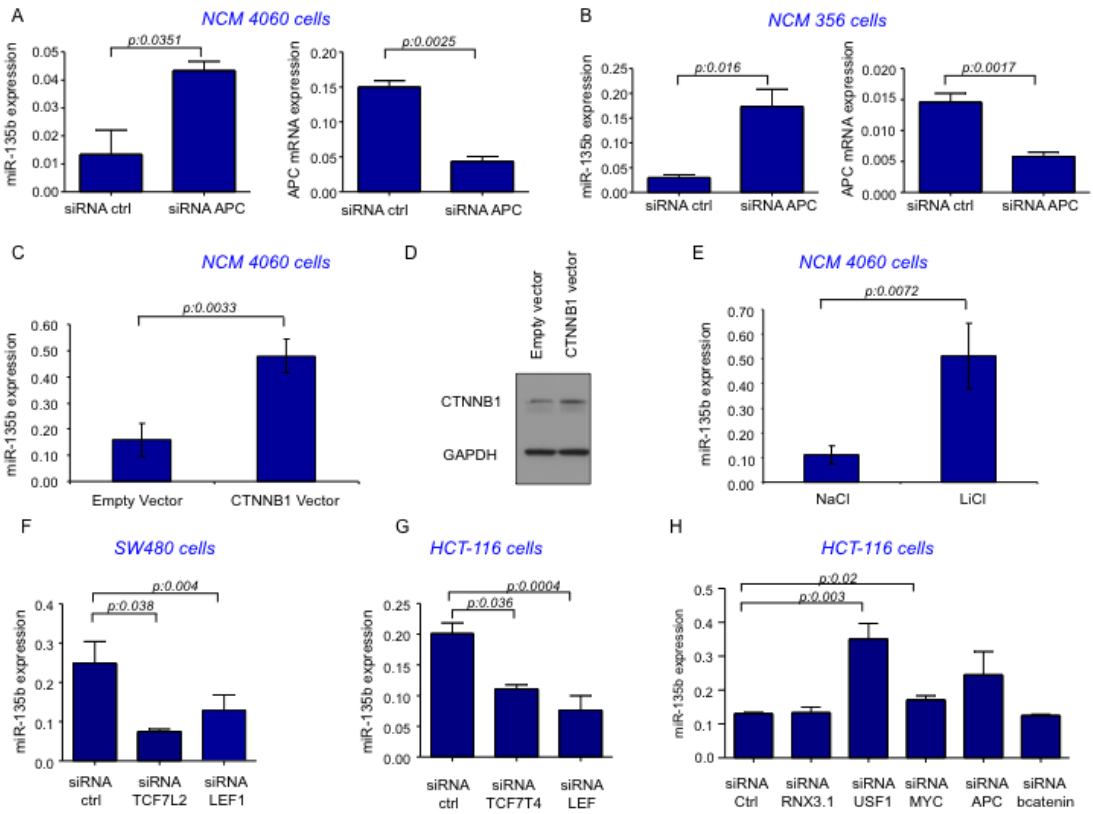

Figure 6. hsa-miR-135b expression was assessed by real time PCR in human CRC cell lines. The expression of miR-135b was normalized to that of RNU48, while that of other genes to GAPDH. Bars represent the mean and SD of 3 experiments. **A&B.** Expression of hsa-miR-135b after transfection with siRNA to APC in NCM 4060 and NCM356 cells. **C&D.** hsa-miR-135b expression after transfection with a vector over-expressing CTNNB1 (β-catenin). **E.** hsa-miR-135b expression after treatment with NaCl and LiCL. **F&G&H.** hsa-miR-135b expression after transfection with selected siRNA as indicated. Statistically significant comparisons are reported.

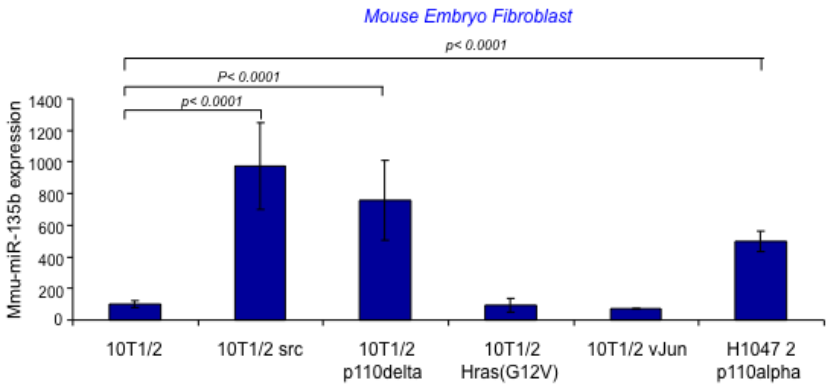

Figure 7. mmu-miR-135b expression was assessed by real time PCR in mouse embryo fibroblasts with genetic aberrations. The expression of miR-135b was normalized to that of SNU234.

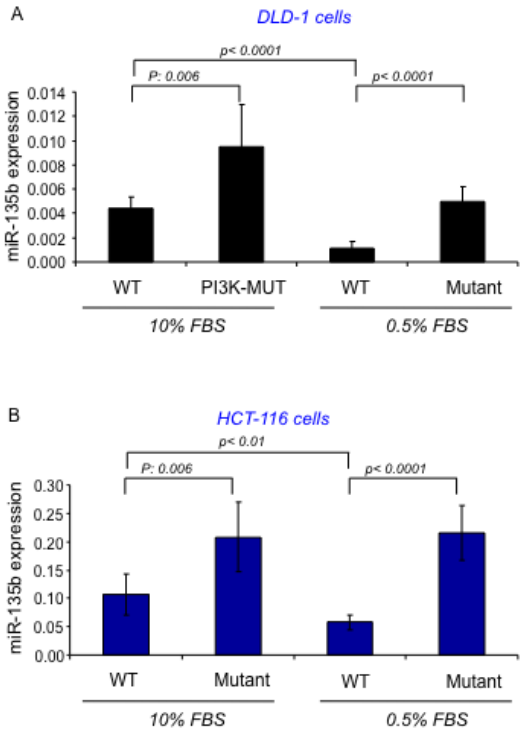

Figure 8. A&B. hsa-miR-135b expression was assessed by real time PCR in human CRC cell lines with or without mutation of the PI3K after exposure to 10% or 0.5% of Fetal Bovine Serum (FBS). Bars represent mean and SD of 3 experiments.

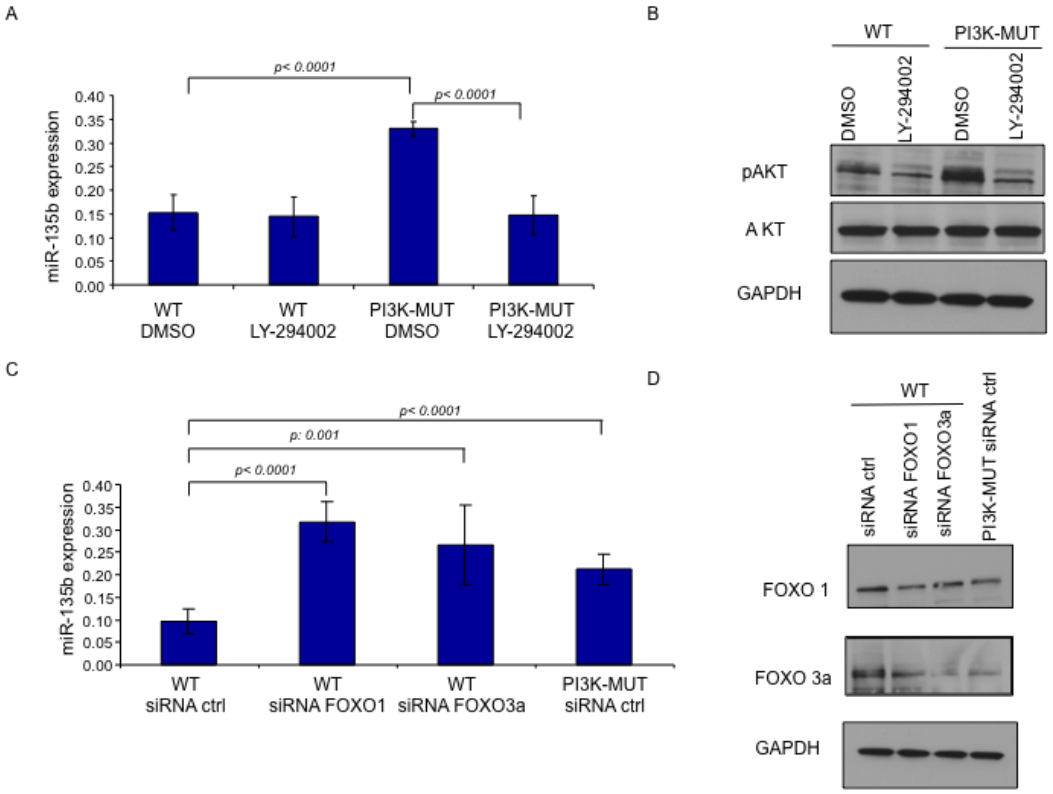

Figure 9. A. hsa-miR-135b expression was assessed by real time PCR in human CRC cell lines with or without mutation of the PI3K after exposure to the PI3K inhibitor (LY-294002). Bars represent mean and SD of 3 experiments. **B.** Inhibition of pAKT by LY-294002. **C.** hsa-miR-135b expression was assessed by real time PCR in human CRC cell lines with or without mutation of the PI3K after transfection with selected siRNAs. Bars represent mean and SD of 3 experiments. **D.** Inhibition of FOXO1 and 3a protein expression by siRNAs.

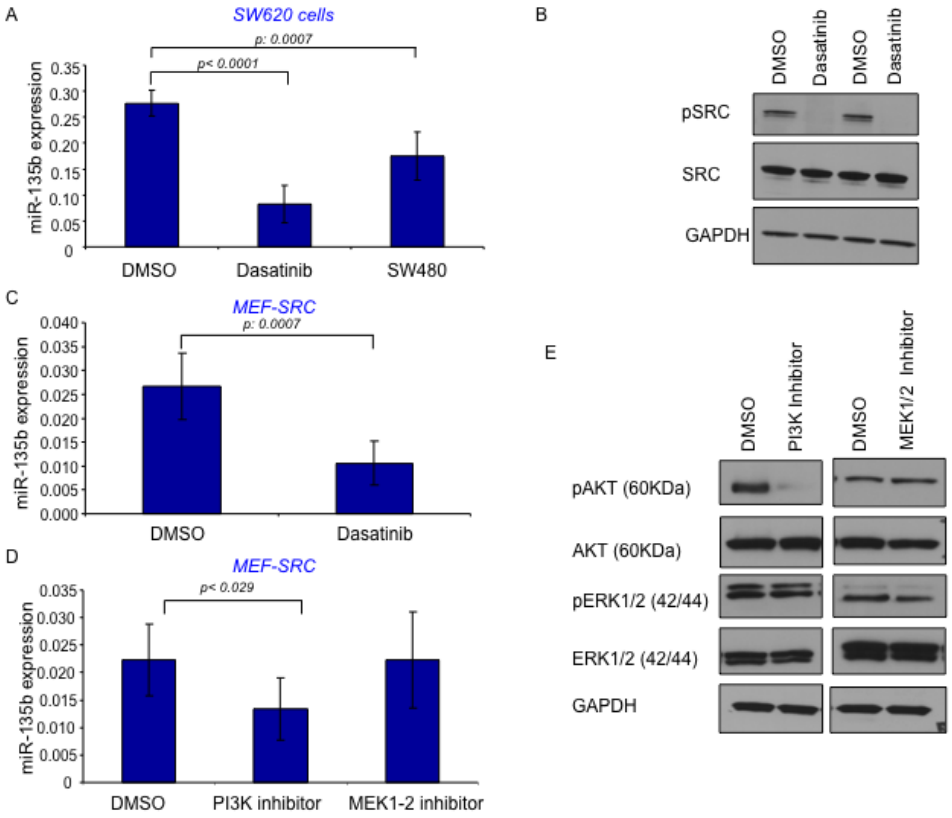

Figure 10. A. hsa-miR-135b expression was assessed by real time PCR in human CRC cell lines after treatment with Dasatinib. Bars represent the mean and SD of 3 experiments. **B.** Inhibition of pSRC by Dasatinib. **C.** mmu-miR-135b expression was assessed by real time PCR in mouse embryo fibroblasts after treatment with Dasatinib. Bars represent the mean and SD of 3 experiments. **D.** mmu-miR-135b expression was assessed by real time PCR in mouse embryo fibroblasts after treatment with PI3K inhbitor and MEK1/2 inhibitor. Bars represent the mean and SD of 3 experiments. **E.** Inhibition of pAKT and pERK respectively in MEF-SRC.

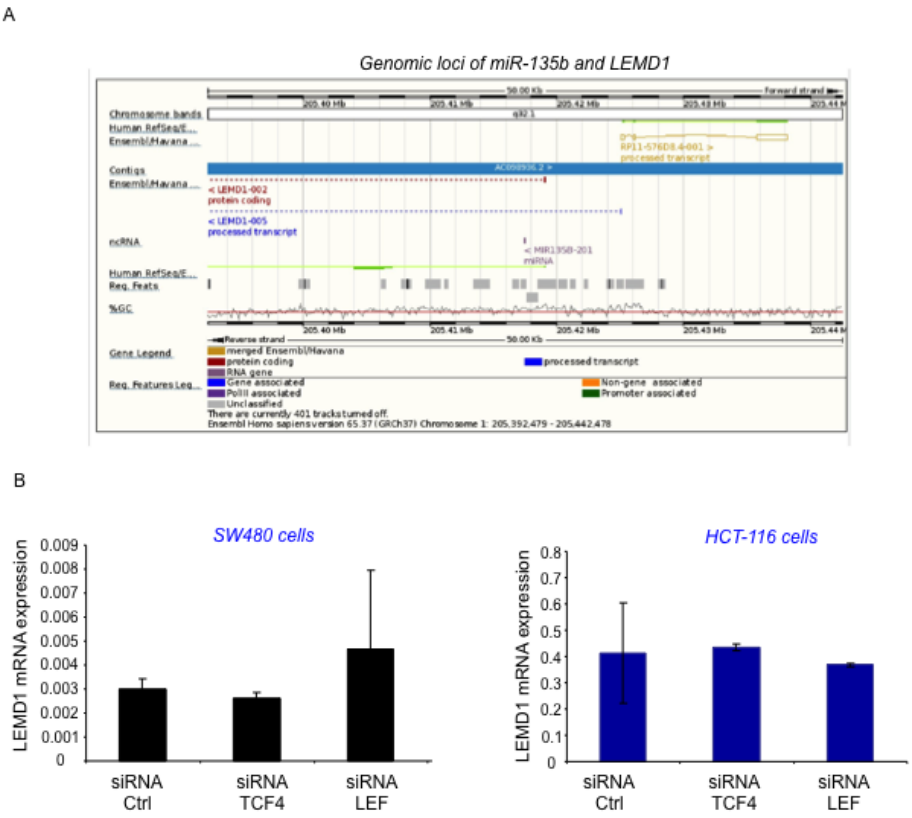

Figure 11. A. Schematic model of the genomic site of hsa-miR-135b. **B.** LEMD1 mRNA expression was assessed by real tIme PCR and normalized to GAPDH.

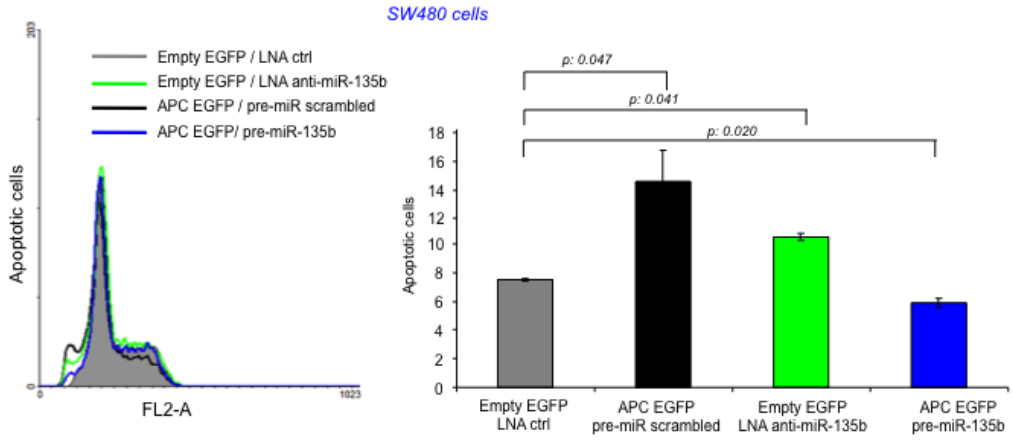

Figure 12. Analysis of apoptosis was performed by flow cytometry. Proportion of propidium iodide positive cells in the different groups of treatment is shown on the left side and quantitated in the right side.

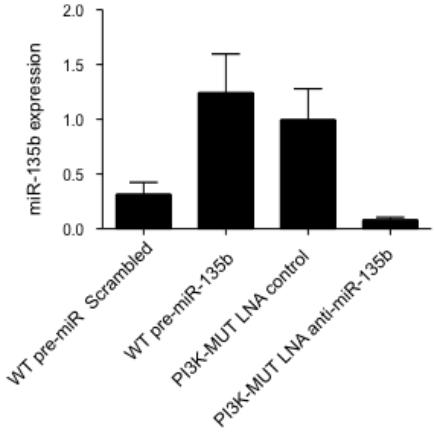

Figure 13. hsa-miR-135b expression was evaluated after transfection with selected probes as indicated.

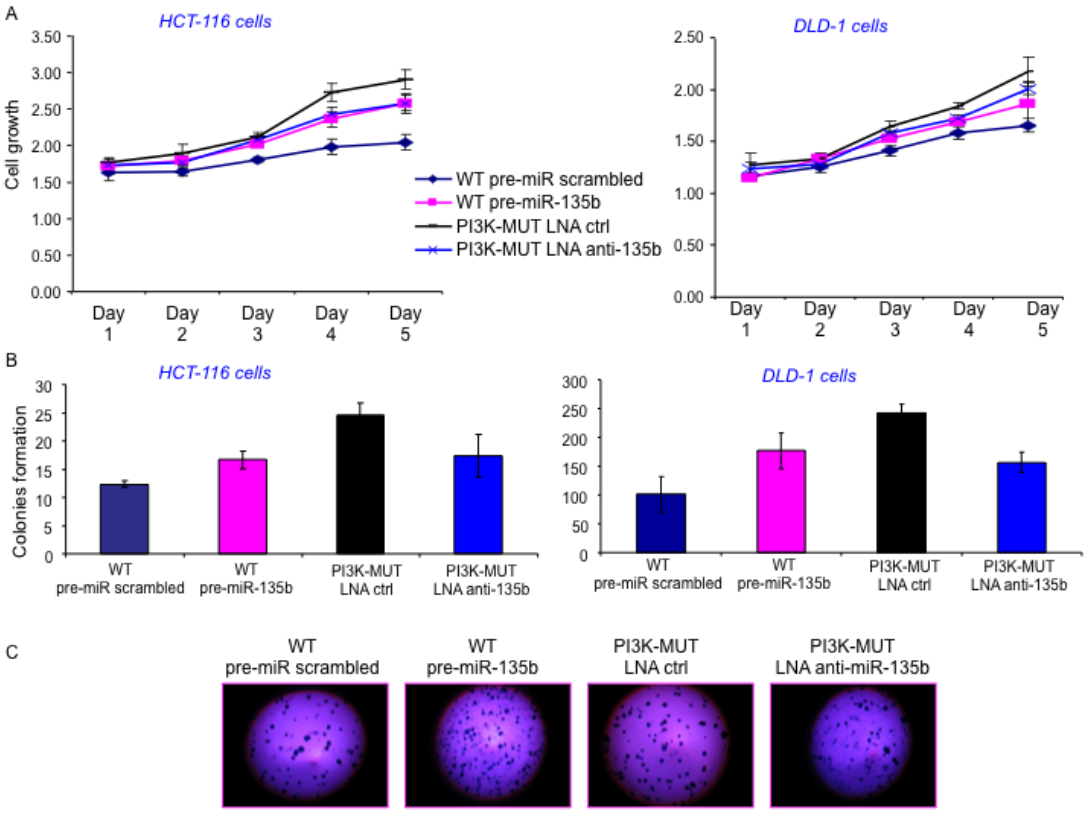

Figure 14. A. Human CRC cells were transfected for 48 hours with selected probes as indicated and then plated. After selected time points cell viability was measured by MTT assay. Mean values of 3 independent experiments with SD are represented. **B&C.** Human CRC cells were transfected for 48 hours with selected probes as indicated and then plated in soft agar. Colonies greater than 2 mm in size were counted and quantitated. Representative images are shown.

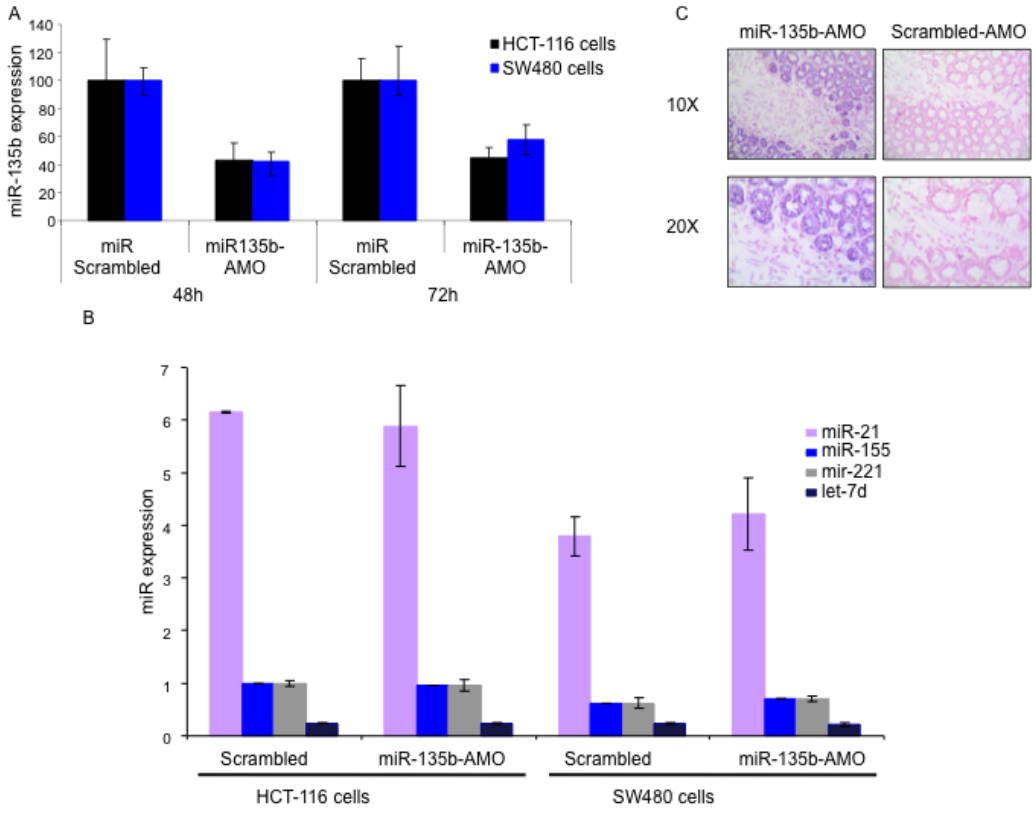

Figure 15. A. Human CRC cell lines were treated with a probe anti-miR-135b (miR-135b-AMO) or a scrambled probe (scrambled-AMO) and miR-135b expression assessed by real time PCR. **B**. expression of miR-21, miR-155, miR-221 and let7-d was evaluated to test 135b-AMO off-target effects. **C.** Mice were treated with miR-135b-AMO or scrambled-AMO and colon tissue collected. ISH was assessed with an anti-anti-miR-135b. Colon tissues were positive to indicate that miR-135b-AMO could reach the colon tissue in vivo.

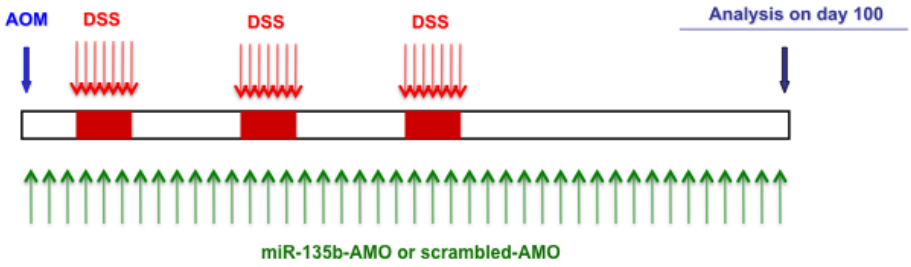

Figure 16. Schematic representation of the mice treatment. AOM was given once, followed by periodic administration of DSS (in water for 7 days ever). miR-135b-AMO or scrambled-AMO was given twice a week from the beginning of treatment for 100 days.

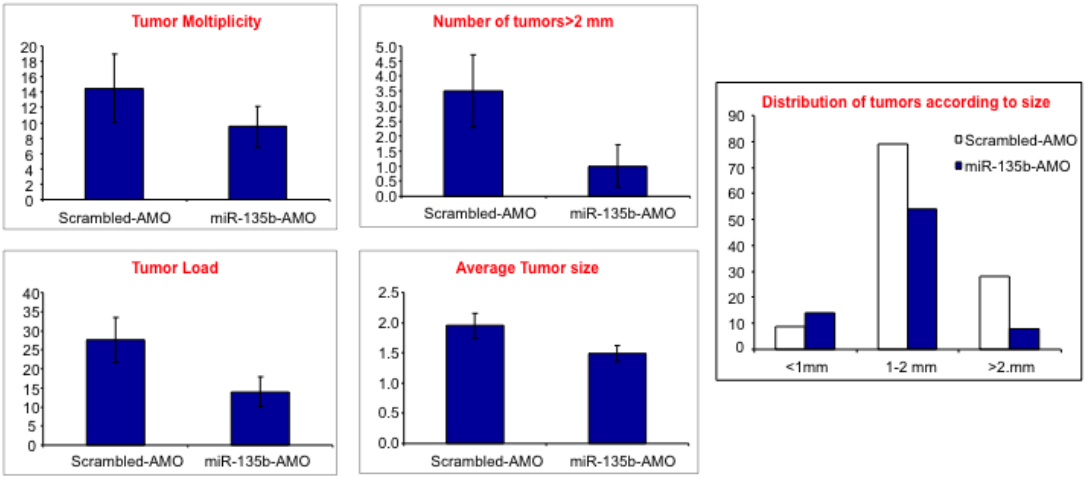

Figure 17. Mice (n=8) were treated with miR-135b-AMO or scrambled-AMO and colon collected and analyzed for presence of tumors. miR-135b-AMO reduced the number and the size of colon tumors.

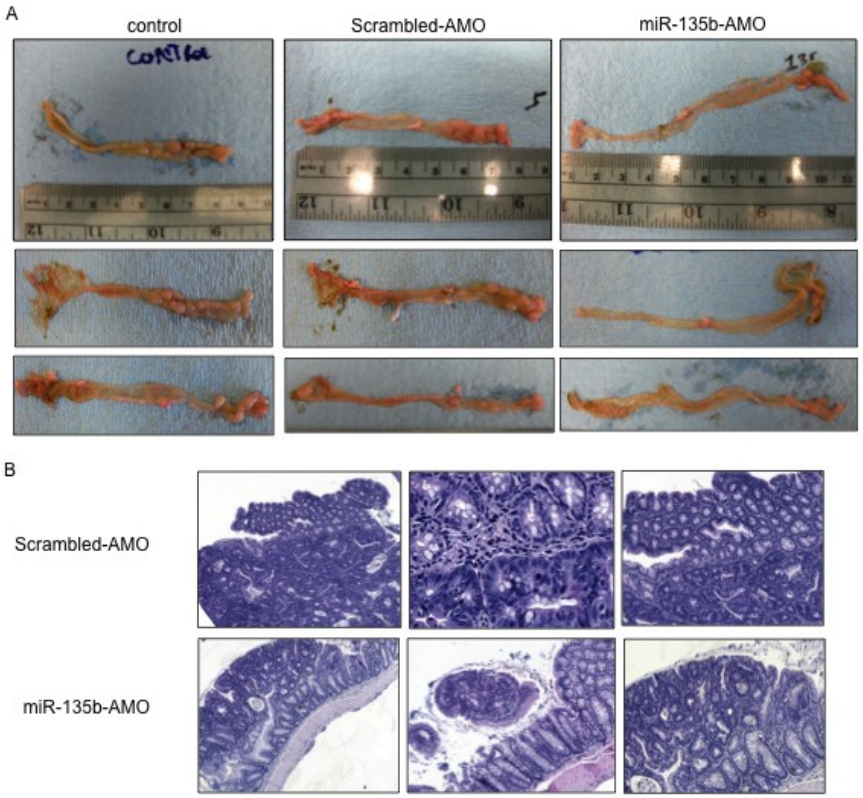

Figure 18. Mice (n=8) were treated with miR-135b-AMO or scrambled-AMO or no treatment (control) and colon collected and analyzed for presence of tumors. Macroscopic (**A**) and microscopic (**B**) representative images are shown.

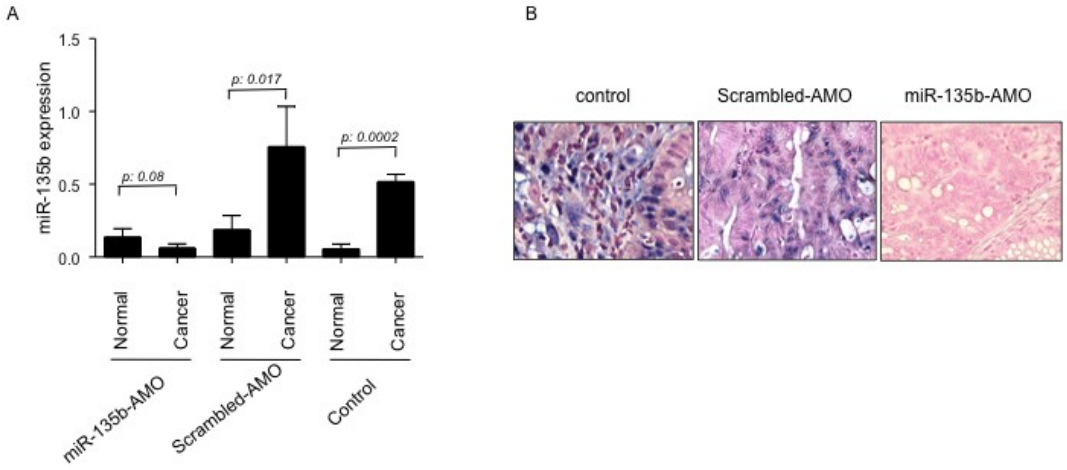

Figure 19. miR-135b expression was assessed by real time PCR (**A**) and ISH (**B**) in cancer tissues from mice treated with miR-135b-AMO or scrambled-AMO or control.

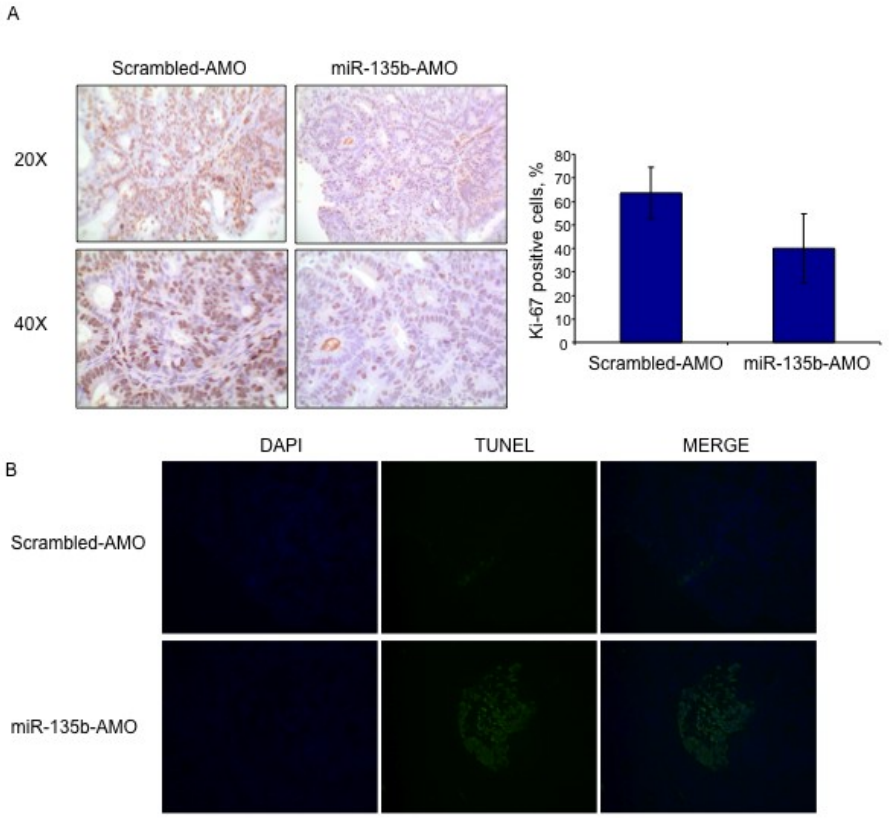

Figure 20. A. Cancer tissues from mice treated with miR-135b-AMO or scrambled-AMO were analyzed by IHC for Ki-67 expression. miR-135b-AMO reduced Ki67 index. **B.** Cancer tissues from mice treated with miR-135b-AMO or scrambled-AMO were analyzed by immunofluorescence for TUNEL and DAPI expression. miR-135b-AMO increased apoptotic (TUNEL positive) cells.

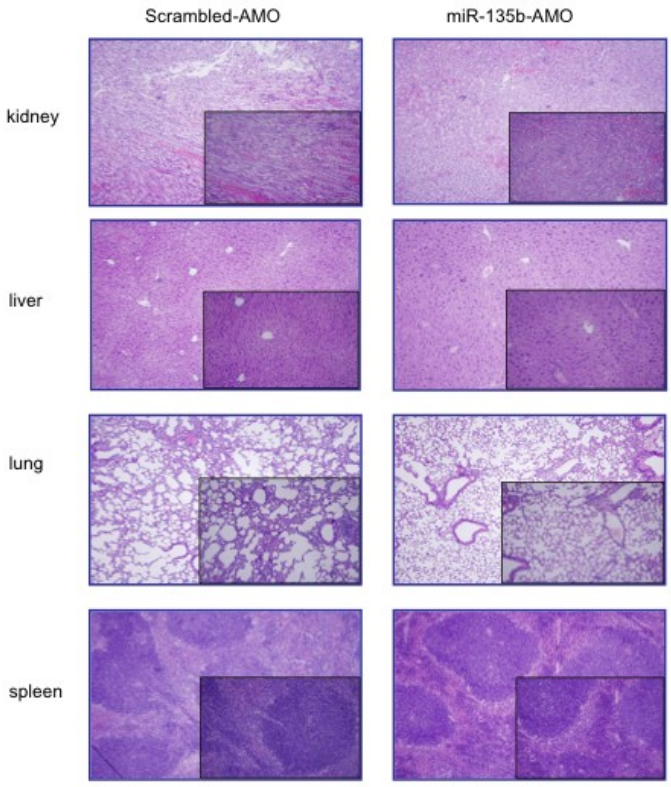

Figure 21. Lungs, livers, kidneys and spleens from miR-135b-AMO and scrambled-AMO treated mice were compared. No differences were found.

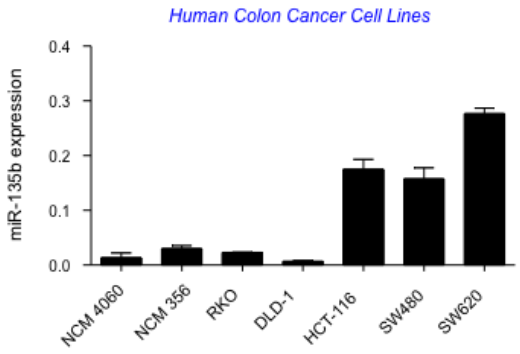

Figure 22. Expression of hsa-miR-135b in a panel of human CRC cell lines. Bars represent mean and SD of 3 samples.

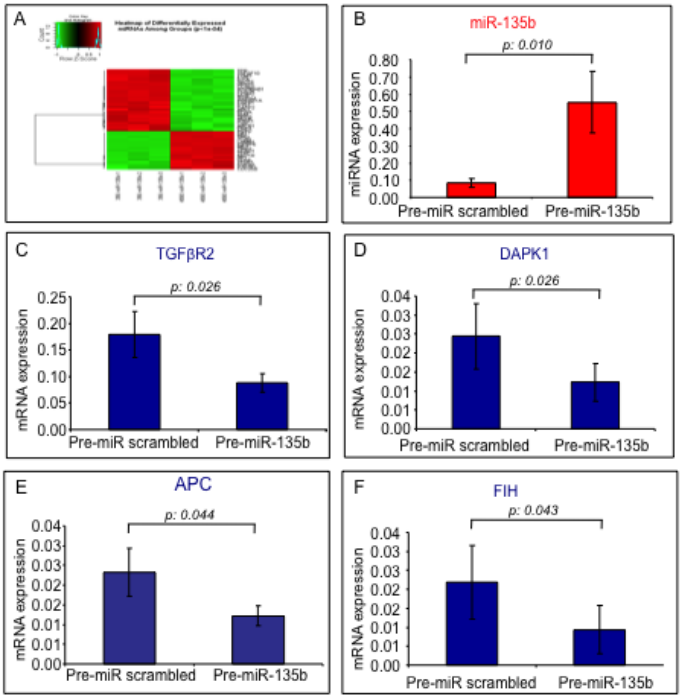

Figure 23. A. Gene expression in 4060NCM cell transfected with pre-miR-135b or scrambled probe. **B&C&D&F** RT-PCR- in NCM4060 cells transfected with pre-miR-135b. Results represent mean and SD of three different experiments.

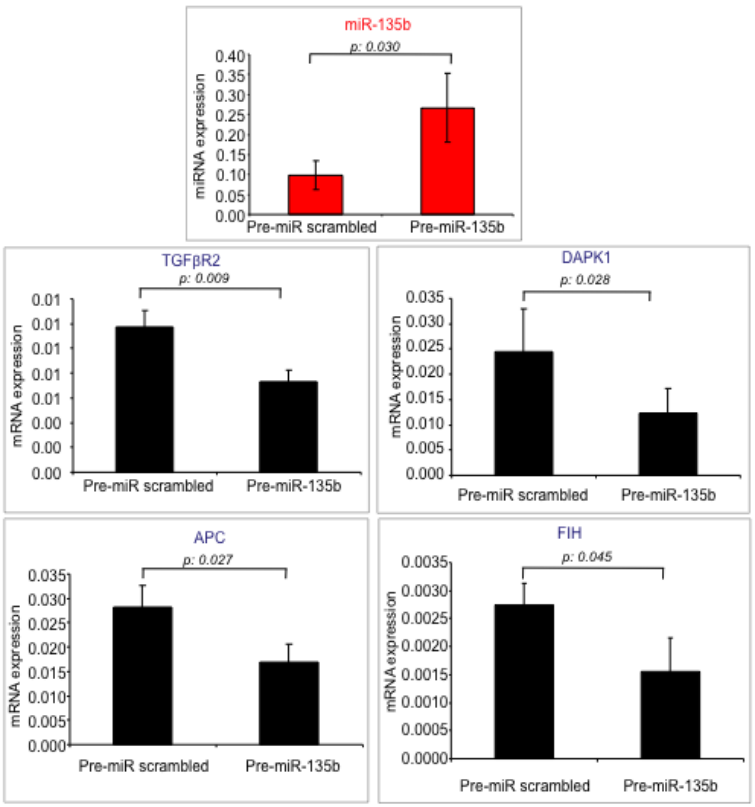

Figure 24. A RT-PCR for miR-135b in NCM4060 transfected cells. RT-PCR for **B** TGFβR2 **C** DAPK1 **D** APC **E** FIH expression in NCM4060 cells over-expressing miR-135b compared to scrambled transfected cells. Results represent mean and SD of three different experiments.

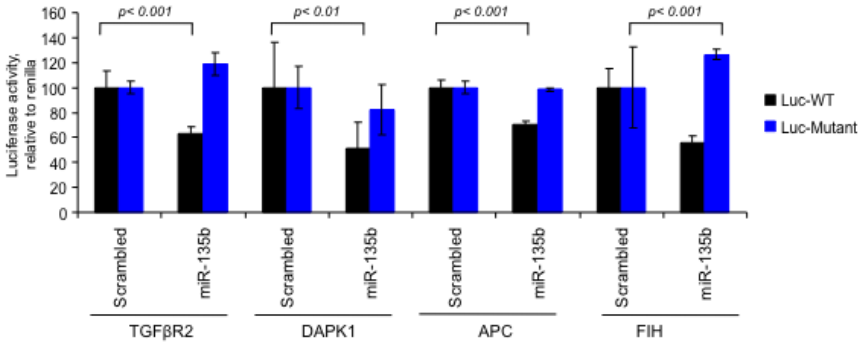

Figure 25. Luciferase experiments for TGFβR2, DAPK1, APC and FIH in NCM4060 transfected with target-gene-Luc-WT or target-gene-Luc-mutant, pre-miR-135b or scrambled miR plus renilla as control. Results represent mean and SD of three different experiments.

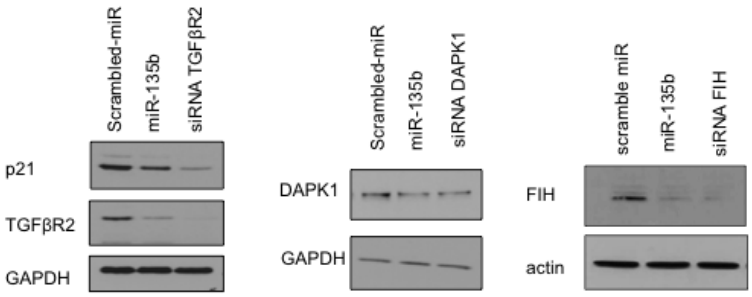

Figure 26. Western blotting analysis in cells transfected with pre-miR-135b or scrambled miR or selected siRNA.